

1 **Parameter regionalization of a monthly water balance model for**
2 **the conterminous United States**

3 **A.R. Bock¹, L.E. Hay², G.J. McCabe², S.L. Markstrom², and R.D. Atkinson³**

4 ¹ U.S. Geological Survey, Colorado Water Science Center, Denver Federal Center, P.O. Box
5 25046, MS 415, Denver, Colorado, 80225, USA

6 ² U.S. Geological Survey, National Research Program, Denver Federal Center, P.O. Box 25046,
7 MS 413, Denver, Colorado, 80225, USA

8 ³ U.S. Environmental Protection Agency, Office of Water (4503-T), 1200 Pennsylvania Ave.,
9 Washington, DC, 20004, USA

10
11 Correspondence to: A. Bock (abock@usgs.gov)

25 **Abstract**

26 A parameter regionalization scheme to transfer parameter values from gaged to ungaged areas
27 for a monthly water balance model (MWBM) was developed and tested for the conterminous
28 United States (CONUS). The Fourier Amplitude Sensitivity Test, a global-sensitivity algorithm,
29 was implemented on a MWBM to generate parameter sensitivities on a set of 109,951 hydrologic
30 response units (HRUs) across the CONUS. The HRUs were grouped into 110 calibration
31 regions based on similar parameter sensitivities. Subsequently, measured runoff from 1,575
32 streamgages within the calibration regions were used to calibrate the MWBM parameters to
33 produce parameter sets for each calibration region. Measured and simulated runoff at the 1,575
34 streamgages showed good correspondence for the majority of the CONUS, with a median
35 computed Nash-Sutcliffe Efficiency coefficient of 0.76 over all streamgages. These methods
36 maximize the use of available runoff information, resulting in a calibrated CONUS-wide
37 application of the MWBM suitable for providing estimates of water availability at the HRU
38 resolution for both gaged and ungaged areas of the CONUS.

39

40

41

42

43

44

45

46

47

48 **1 Introduction**

49 The WaterSMART program (<http://water.usgs.gov/watercensus/WaterSMART.html>) was started
50 by the United States (U.S.) Department of the Interior in February 2010. Under WaterSMART,
51 the National Water Census (NWC) was proposed as one of the U.S. Geological Survey's (USGS)
52 key research directions with a focus on developing new hydrologic tools and assessments. One
53 of the major components of the NWC is to provide estimates of water availability at a sub-
54 watershed resolution nationally (<http://water.usgs.gov/watercensus/streamflow.html>) with the
55 goal of determining: (1) if the Nation has enough freshwater to meet both human and ecological
56 needs and (2) if this water will be available to meet future needs. Streamflow measurements do
57 not provide direct observations of water availability at every location of interest; approximately
58 72 percent (%) of land within the conterminous U.S. is gaged, with approximately 13% of these
59 gaged areas being unaffected by anthropogenic effects (Kiang et al., 2013). This creates the
60 challenge of determining the best method to transfer information from gaged catchments to data-
61 poor areas where results cannot be calibrated or evaluated with measured streamflow (Vogel,
62 2006). This transfer of model parameter information from gaged to ungaged catchments is
63 known as hydrologic regionalization (Bloschl and Sivapalan, 1995).

64 Many hydrologic regionalization methods have focused on developing measures of similarity
65 between gaged and ungaged catchments using spatial proximity and physical characteristics.
66 These methods are highly dependent on the complexity of the terrain and scale at which the
67 relations are derived. Spatial proximity is considered the primary explanatory variable for
68 hydrologic similarity (Sawicz et al., 2011) because of the first-order effects of climatic and
69 topographic controls on hydrologic response. Close proximity, however, does not always result
70 in hydrologic similarity (Vandewiele and Elias, 1995; Smakhtin, 2001; Ali et al., 2012).

71 Physical characteristics have been used as exploratory variables to develop a better
72 understanding of the relation between model parameters that represent model function, and
73 physical properties of the catchment (Merz and Bloschl, 2004). The relation between model
74 parameters and the relevant physical characteristics, expressed for example as a form of
75 multivariate regression, can be transferred to ungaged catchments (Merz and Bloschl, 2004).
76 Model parameter definitions are by nature ambiguous and often difficult to correlate to a small

77 number of meaningful variables such as physical and climatic characteristics (Zhang et al.,
78 2008); some studies have found no significant correlation between catchment attributes and
79 model parameters (Seibert, 1999; Peel et al., 2000), whereas others found that high correlation
80 does not guarantee parameters that result in reliable model simulations of measured data (Sefton
81 and Howarth, 1998; Kokkonen et al., 2003; Oudin et al., 2010). Physical and hydrologic
82 characteristics also are used to derive measures of similarity (or dissimilarity) from multi-
83 dimensional attribute space, which can be used to identify donor catchments (Qamar et al.,
84 2015), or classify catchments into discrete regions or clusters (Oudin et al., 2008, 2010; Samuel
85 et al., 2011). While these methods have indicated some success in simulating behavior of
86 specific hydrologic components, such as base flow (Santhi et al., 2008) or monthly flow regimes
87 (Qamar et al., 2015), other efforts utilizing discrete clusters performed poorly in explaining
88 variability of measured streamflow (McManamay et al., 2011).

89 Two important components of the transfer of parameters to ungauged catchments are the
90 identification of (1) influential (and non-influential) parameters, and (2) geographic extents and
91 scales at which parameters exert control on model function. Reducing the number of parameters
92 is important for calibration efficiency by reducing the structural bias of the model and the
93 uncertainty of results where they cannot be verified or confirmed (Van Griensven et al., 2006). A
94 high number of calibrated, poorly constrained parameters can often mask data or structural
95 errors, which can go undetected and reduce the skill of the model in replicating results outside of
96 calibration conditions (Kirchner, 2006; Bloschl et al., 2013; Bárdossy et al., 2015). This
97 increases the potential for equifinality of parameter sets and higher model uncertainty that can be
98 propagated to model results (Troch et al., 2003).

99 Sensitivity analysis (SA) has advanced the understanding of parameter influence on model
100 behavior and structural uncertainty. SA measures the response of model output to variability in
101 model input and/or model parameter values. SA partitions the total variability in the model
102 response to each individual model parameter (Reusser et al., 2011) and results in a more-defined
103 set of parameters and parameter ranges. Identification of sensitive parameters and their ranges is
104 important for hydrologic model applications as key model parameters can vary spatially across
105 physiographic regions, and also temporally (Tang et al., 2007; Guse et al., 2013).

106 Until recently, the high computational demands of SA have limited most implementations of
107 hydrologic model SA to local sensitivity algorithms that evaluate a single parameter at a time
108 (Tang et al., 2007). Global SA uses random or systematic sampling designs of the entire
109 parameter space to quantify variation in model output (Van Griensven et al. 2006, Reusser et al.
110 2011). Some of these methods can account for parameter interaction and quantify sensitivity in
111 non-linear systems. Global SA methods are computationally intensive (Cuo et al., 2011), but
112 ever increasing computational efficiency has allowed for the development and application of a
113 large number of global SA algorithms.

114 Previous work has suggested that isolating the key parameters that control model performance
115 can be used to infer dominant physical processes in the catchment, as well as which components
116 of the model dominate hydrologic response (Van Griensven et al. 2006, Tang et al., 2007,
117 Reusser et al., 2011). To date, there has been little analysis of the use of SA for deriving
118 measures of hydrologic similarity across catchments that can be applied towards hydrologic
119 regionalization of model parameters. The spatially-distributed application of SA could be used
120 to provide additional information for the delineation of homogeneous regions for parameter
121 transfer based on similarity of model results from the SA. This strategy allows for the use of the
122 existing model information and configuration to develop a calibration and regionalization
123 framework without significantly changing the model structure or implementation

124 In this study, we present a hydrologic regionalization methodology for the CONUS that derived
125 regions of hydrologic similarity based on the response of a Monthly Water Balance Model
126 (MWBM) to parameter SA. Groups of streamgages within each region are calibrated together to
127 define a single parameter set for each region. By extending model calibration to a large number
128 of sites grouped by similarity through a quantified measure of model behavior, a more specific
129 and constrained parameter space that fits each region can be identified.

130 **2 Methods**

131 **2.1 Monthly Water Balance Model**

132 The MWBM (Fig. 1) is a modular accounting system that provides monthly estimates of
133 components of the hydrologic cycle by using concepts of water supply and demand (Wolock and

134 McCabe, 1999; McCabe and Markstrom, 2007). Monthly temperature (T) is used to compute
135 potential evapotranspiration (PET) and to partition monthly precipitation (P) into rain and snow
136 (Fig. 1). Precipitation that occurs as snow is accumulated in a snow pack (snow storage as snow
137 water equivalent, or SWE); rainfall is used to compute direct runoff (R_{direct}) or overland flow,
138 actual evapotranspiration (AET), soil-moisture storage recharge, and surplus water, which
139 eventually becomes runoff (R) (Fig. 1). When rainfall for a month is less than PET, AET is equal
140 to the sum of rainfall, snowmelt, and the amount of moisture that can be removed from the soil.
141 The fraction of soil-moisture storage that can be removed as AET decreases linearly with
142 decreasing soil-moisture storage; that is, water becomes more difficult to remove from the soil as
143 the soil becomes drier and less moisture is available for AET. When rainfall (and snowmelt)
144 exceeds PET in a given month, AET is equal to PET; water in excess of PET replenishes soil-
145 moisture storage. When soil-moisture storage reaches capacity during a given month, the excess
146 water becomes surplus and a fraction of the surplus (R_{surplus}) becomes R , while the remainder of
147 the surplus is temporarily held in storage. The MWBM has been previously used to examine
148 variability in runoff over the CONUS (Wolock and McCabe, 1999; Hay and McCabe, 2002;
149 McCabe and Wolock, 2011a) and the global extent (McCabe and Wolock, 2011b). Table 1 lists
150 the MWBM parameters, with definitions and parameter ranges for calibration.

151 The Ppt_{adj} and Tav_{adj} parameters specify seasonal adjustments for precipitation and
152 temperature, respectively. The seasonal adjustment parameters were included to account for
153 errors in the precipitation and temperature data used in this analysis. Sources of systematic and
154 non-systematic errors of climate forcing data are well documented from the precipitation gage-
155 derived sources (Groisman and Legates, 1994; Adam and Lettenmaier, 2003). Interpolation of
156 these systematic errors from point-scale to gridded domains may propagate these biases,
157 especially in complex terrain (Clark and Slater, 2006; Oyster et al., 2015). The use of adjustment
158 factors allows uncertainty associated with forcing data and model parameter values to be treated
159 separately (Vrugt et al., 2008).

160 *Figure 1. Conceptual diagram of the Monthly Water Balance Model (McCabe and Markstrom*
161 *2007). Processes influenced by model parameters used in Fourier Amplitude Sensitivity Test*
162 *(FAST) are identified by green arrow and numbered (Table 1).*

163 Table 1. [Monthly Water Balance Model parameters and ranges.](#)

164 The MWBM was applied to the CONUS with 109,951 hydrologic response units (HRUs) from
165 the Geospatial Fabric (Viger and Bock, 2014), a national database of hydrologic features for
166 national hydrologic modeling applications (Fig. 2). This HRU derivation is based on an
167 aggregation of the NHDPlus dataset (USEPA and USGS, 2010), an integrated suite of geospatial
168 data that incorporates features from the National Hydrography Dataset (<http://nhd.usgs.gov/>), the
169 National Elevation Dataset (<http://ned.usgs.gov/>), and the Watershed Boundary Dataset
170 (<http://nhd.usgs.gov/wbd.html>). The sizes of the HRUs range from less than 1 square kilometer
171 (km^2) up to 67,991 km^2 , with an average size of 74 km^2 .

172 Inputs to the MWBM by HRU are: (1) monthly P (millimeters), monthly mean T (degrees
173 Celsius), (2) latitude of the site (decimal degrees), (3) soil moisture storage capacity
174 (millimeters), and (4) monthly coefficients for the computation of PET (dimensionless).
175 Monthly P and mean T were derived from the daily time step, $1/8^\circ$ gridded meteorological data
176 for the period of record from January 1949 through December 2011 (Maurer et al., 2002).
177 Monthly P and T data were aggregated for each HRU using the USGS Geo Data Portal
178 (<http://cida.usgs.gov/climate/gdp/>) (Blodgett et al., 2011). Latitude was computed from the
179 centroid of each HRU. Soil moisture storage capacity was calculated using a 1 km^2 grid derived
180 from the Soils Data for the Conterminous United States (STATSGO) (Wolock, 1997). The
181 monthly PET coefficients were calculated by calibrating the Hamon PET values to Farnsworth et
182 al. (1982) mean monthly free-water surface evapotranspiration. McCabe et al. (2015) describes
183 these PET coefficient calculations in detail.

184 *Figure 2. Hydrologic Response Units of the Geospatial Fabric, differentiated by color, overlain*
185 *by NHDPlus region boundaries (R01-R18).*

186 **2.2 Fourier Amplitude Sensitivity Test**

187 A parameter SA for the CONUS was conducted for the MWBM using the Fourier Amplitude
188 Sensitivity Test (FAST) to identify areas of hydrologic similarity. FAST is a variance-based
189 global sensitivity algorithm that estimates the contribution to model output variance explained by
190 each parameter (Cukier et al. 1973, 1975; Saltelli et al. 2000). Advantages of using FAST over

191 other SA methods are that FAST can calculate sensitivities in non-linear systems, and is
192 extremely computationally efficient. The seasonal adjustment factors were not incorporated in
193 the FAST analysis. We viewed the seasonal adjustment factors as related more to the forcing
194 data, and for this application only parameters associated with model structure were included
195 (first five parameters in Table 1).

196 FAST transforms a model's multi-dimensional parameter space into a single dimension of
197 mutually independent sine waves with varying frequencies for each parameter, while using the
198 parameter ranges to define each wave's amplitude (Cukier et al., 1973, 1975; Reusser et al.,
199 2011). This methodology creates an ensemble of parameter sets numbering from 1 to N, each of
200 which is unique and non-correlated with the other sets. Parameter sets are derived using the
201 corresponding y-values along each parameter's sine wave given a value on the x-axis. The
202 model is executed for all parameter sets using identical climatic and geographic inputs for each
203 simulation. The resulting series of model outputs are Fourier-transformed to a power spectrum
204 of frequencies for each parameter. Parameter sensitivity is calculated as the sum of the powers
205 of the output variance for each parameter, divided by the sum of the powers of all parameters
206 (Total Variance). The parameter sensitivities are scaled so that the sensitivities for all
207 parameters sum to 1. Thus, parameters that explain a large amount of variability in the model
208 output have higher values of (i.e. closer to 1) parameter sensitivity values.

209 FAST was implemented with the MWBM using the 'fast' library in the statistical software R
210 (Reusser, 2012; R Core Team, 2013). Parameter ranges used by FAST for generating wave
211 amplitudes of parameter ensembles across the CONUS were based on table 1. The 'fast' R
212 package pre-determines the minimal number of runs necessary to estimate the sensitivities for
213 the given number of parameters (Cukier et al., 1973). For our application we generated an
214 ensemble of 1000 parameter sets (as compared to the minimally suggested number of 71
215 estimated by 'fast') to have the capability to compare results of different sensitivity analysis
216 methods. The computational efficiency of the MWBM allowed the parameter sets to be
217 simulated quickly through parallel processing.

218 Many applications of SA in hydrologic modeling have evaluated parameter sensitivity for
219 measured streamflow using performance-based measures such as bias, root mean squared error

220 (RMSE), and the Nash-Sutcliffe Efficiency (NSE) (Nash and Sutcliffe, 1970; Moriasi et al.,
221 2007). In this study, parameter sensitivity is examined using two hydroclimatic indices that
222 account for the magnitude and variability of both climatic input and model output: the (1) Runoff
223 Ratio (RR), a ratio of simulated runoff to precipitation, and (2) Runoff Variability (RV) index,
224 the standard deviation of simulated runoff to the standard deviation of precipitation
225 (Sankarasubramanian and Vogel, 2003).

226 **3 Parameter regionalization procedure**

227 The MWBM parameter sensitivities from the FAST analysis using an ensemble of 1000 MWBM
228 parameter sets were evaluated across the CONUS. The spatial patterns and magnitudes of
229 parameter sensitivities then were used to organize the 109,951 HRUs across the CONUS into
230 hydrologically similar regions for parameter regionalization through MWBM calibration.
231 Potential streamgages were identified for use in two automated calibration procedures. The
232 calibration procedures were used to produce an ‘optimal’ set of MWBM parameters for each
233 calibration region. The following sections describe the parameter regionalization procedure in
234 detail (Fig. 3).

235 *Figure 3. Schematic flowchart of the parameter sensitivity analysis and regionalization method*
236 *described in this paper (Section 3).*

237 **3.1 Parameter sensitivities**

238 The relative sensitivities derived from the FAST analysis using the RR and RV indices at each of
239 the 109,951 HRUs across the CONUS were scaled so that the five MWBM parameter
240 sensitivities derived for each HRU summed to 100 (Fig. 4). RR (Fig. 4a) is most sensitive to the
241 parameter *Drofac* in regions where MWBM runoff is not dominated by snowmelt and orographic
242 precipitation, such as arid and sub-tropical areas of the CONUS. MWBM parameters that
243 control snowpack accumulation and melt (*Meltcoef*, *Tsnow*, and *Train*) are more important to the
244 RR in the extensive mountain ranges in the Western CONUS, and northerly latitudes around the
245 Great Lakes and in the Eastern CONUS. The RR indicates the highest sensitivity to the *Rfactor*
246 parameter in mountainous areas of the CONUS and areas of the West Coast, and moderate to
247 high sensitivity in areas where the sensitivity of RR to *Drofac* is low. *Tsnow*, *Train*, and

248 *Meltcoef* all share similar patterns across the CONUS. The spatial variability of the sensitivity of
249 RR to *Meltcoef* indicates different physical mechanisms controlling *Meltcoef* parameter influence
250 on RR in different areas of the CONUS. In the Western CONUS, the sensitivity of RR to
251 *Meltcoef* is greatest in mountainous areas that accumulate and hold snowpack through the late
252 spring, such as the Rocky Mountains, Cascade, and Sierra Nevada mountain ranges. In the
253 Eastern and Midwestern CONUS, the sensitivity of RR to *Meltcoef* is greatest for HRUs with
254 more northerly latitudes.

255 *Figure 4. Relative sensitivity of the (a) Rainfall Ratio (RR) and (b) Runoff Variability (RV)*
256 *indices to Monthly Water Balance Model parameters.*

257 The spatial patterns of sensitivities of RV to the five MWBM parameters (Fig. 4b) show both
258 similarities and deviations from the patterns shown in the RR maps. For the central part of the
259 CONUS, the relative sensitivity for the parameter *Drofac* is high for both indices, and low for the
260 parameter *Rfactor* for both indices. *Meltcoef*, *Tsnow*, and *Train* share the same relations between
261 higher sensitivity and higher elevation (primarily in the western part of the CONUS), and higher
262 sensitivity and more northerly latitude (primarily in the eastern half of the CONUS) for both
263 indices. However, *Drofac* and *Rfactor* show distinctly different patterns of relative sensitivities
264 for the eastern part of the CONUS for RV as compared to RR. The other three parameters
265 follow the same general spatial patterns for RV as compared to RR, but with greater fine-scale
266 spatial variation and patchiness. The differences between the spatial distributions of the
267 sensitivities between the two indices highlight that applying SA to different model outputs can
268 generate different levels of sensitivities for each parameter. In addition, the choice of objective
269 function or model output for which to measure parameter sensitivity is important, as parameter
270 sensitivities will differ depending on whether a user evaluating measures of magnitude, the
271 variability of distribution, or timing (Krause et al., 2005; Kapangaziwiri et al., 2012).

272 Figure 5 illustrates the variability of parameter sensitivities between NHDPlus regions 08 (Lower
273 Mississippi) and 14 (Upper Colorado) (see Fig. 2) for the RV and RR indices. The Lower
274 Mississippi and Upper Colorado NHDPlus regions have a similar number of HRUs (4,449 and
275 3,879, respectively) and cover a similar area (26,285 and 29,357 km², respectively). The Lower
276 Mississippi region has homogenous topography, with humid, subtropical climate, while the

277 Upper Colorado region has highly variable topography, and thus highly variable climatic
278 controls on hydrologic processes. For the Lower Mississippi region only one parameter
279 dominates modeled RV variance (*Rfactor*, Fig. 5a) and modeled RR variance (*Drofac*, Fig. 5c).
280 In contrast, for the Upper Colorado River region several parameters influence RV variability
281 (*Drofac*, *Rfactor* and *Meltcoef*, Fig. 5b) and RR variability (*Drofac* and *Meltcoef*, Fig. 5d). In
282 the Lower Mississippi Region, the amount of snowfall is negligible, so the three parameters that
283 control snowfall and snowpack accumulation in the MWBM have negligible effect on simulated
284 total runoff. The comparison of the parameter sensitivities for these two regions illustrates how
285 variable parameter sensitivities are for different regions (i.e. different climatic and physiographic
286 regions)

287 *Figure 5. Parameter sensitivities of Runoff Variability (RV; a-b) and Runoff Ratio (RR; c-d)*
288 *indices for Monthly Water Balance Model parameters in the Lower Mississippi (R08) and*
289 *Upper Colorado (R14).*

290 **3.2. Calibration regions**

291 The spatial patterns and magnitudes of parameter sensitivities across the CONUS were used as a
292 basis for organizing HRUs into hydrologically similar regions for parameter regionalization
293 through MWBM calibration. This idea is rooted in the hypothesis that geographically proximate
294 HRUs share similar forcings and conditions, and thus will behave similarly. This application
295 uses similarity in SA results as a basis for organization, rather than similarity in physiographic
296 characteristics. The derived regions are subsequently used to simplify model calibration across
297 the CONUS and provide a basis for the transfer and application of parameters to ungaged areas.

298 The parameter sensitivities derived from the RR were used to organize the HRUs into two
299 independently-derived calibration regions; the first derived by identifying HRUs with unique
300 combinations of the order of parameter sensitivities to the RR (highest parameter sensitivities to
301 lowest, i.e. 1-*Drofac* (78%), 2-*Rfactor* (16%), 3-*Meltcoef* (4%), 4-*Tsnow* (1%), 5-*Train* (1%)),
302 and the second classification based upon identifying HRUs with unique sets of parameters whose
303 sensitivities exceeded a specified threshold of parameter sensitivity (i.e. only *Drofac* and *Rfactor*
304 using a 5% threshold in the first classification example). This classification identified 16 distinct

305 regions of HRUS across the CONUS based on the order of the parameter sensitivities of the five
306 parameters (derived using the RR index). Sizes of these regions ranged from 94 km² to almost 2
307 million km². The second classification delineated regions with an identical set of the most
308 important parameters to the RR based on parameters whose sensitivities exceeded a 5%
309 threshold. This step identified 12 regions of HRUs with unique combinations of parameter
310 sensitivities exceeding 5%. There has been progress in providing quantitative thresholds for the
311 identification of sensitive and non-sensitive parameters for hydrologic modelers (Tang et al.,
312 2007), but no definitive consensus yet exists. Therefore a 5% threshold was used based on visual
313 delineation of major physiographic features such as mountain ranges across the CONUS. The
314 sizes of this second group of regions ranged from 94 km² to more than 15 million km². Maps of
315 the two groupings of HRUS were intersected to create a total of 49 regions across the CONUS.
316 NHDPlus region boundaries, proximity, and significant topographic divides were used to further
317 divide the groups into 159 geographically unique calibration regions across the CONUS. The
318 lack of streamgages available in some regions, especially areas with arid and semi-arid climates,
319 necessitated merging regions together. Calibration regions that contained less than 3
320 streamgages from the 8,410 gages present in the Geospatial Fabric (see section 3.3) were
321 combined with the proximate and most similar group which shared the most similar parameter
322 sensitivities (both order and magnitude), resulting in 110 calibration regions across the CONUS
323 (Fig. 6). Within each region the FAST results for both the RR and RV indices were used to
324 determine which parameters to calibrate. Parameters with a median parameter sensitivity of 5%
325 for the RR and RV among the region's HRUs were selected for group calibration. Parameters
326 not shown as sensitive were kept at the default value for the group.

327 *Figure 6. Final 110 Monthly Water Balance Model calibration regions differentiated by colors.*
328 *A subset of streamgages within each calibration region were calibrated in a group-wise*
329 *fashion to produce a single optimized parameter set for the entire region (Fig. 3).*

330 **3.3 Initial streamgage selection**

331 The initial set of streamgages used for testing in the MWBM calibration procedures was selected
332 from 8,410 streamgages identified in the Geospatial Fabric (Fig. 7). The Geospatial Fabric
333 includes reference and non-reference streamgages from the Geospatial Attributes of Gages for

334 Evaluating Streamflow dataset (GAGES-II, Falcone et al., 2010). Of the 8,410 streamgages in
335 the Geospatial Fabric, 1,864 were identified as having reference-quality data with at least 20
336 years of record. These reference quality streamgages were judged to be largely free of human
337 alterations to flow (Falcone et al., 2010). In the current study, reference quality was not
338 considered in the initial streamgage selection because the 20 years of record was considered too
339 restrictive. Therefore a subset of the 8,410 streamgages was selected for initial testing in the
340 MWBM calibration procedures based on the following criteria:

341 (1) Remove streamgages with less than 10 years of total measured streamflow (120 months)
342 within the time period 1950 – 2010.

343 (2) Remove streamgages with a drainage area defined by the Geospatial Fabric that are not
344 within 5% of the USGS National Water Information System (NWIS) reported drainage
345 area (U.S. Geological Survey, 2014). This eliminated many of the streamgages with
346 smaller drainage areas due to the resolution of the Geospatial Fabric.

347 (3) Remove streamgages that did not have at least 75% of its drainage area contained within
348 a single calibration region.

349 These criteria resulted in 5,457 potential streamgages for testing in the MWBM calibration
350 procedures (Fig. 7). Streamflow at these streamgages was aggregated and converted from daily
351 (cubic feet/second) to a monthly runoff depth (mm) (streamflow per unit area).

352 *Figure 7. Streamgages tested in the study. GF notes geospatial fabric for national hydrologic*
353 *modeling (Viger and Bock, 2014).*

354 **3.4 Monthly Water Balance Model calibration**

355 Two automated calibration procedures were implemented to produce an ‘optimal’ set of MWBM
356 parameters for each calibration region. The first procedure, Individual Streamgage Calibration,
357 calibrated each of the 5,457 streamgages individually. Results from the individual calibrations
358 were used to further filter the streamgages within the second procedure, Grouped Streamgage
359 Calibration, which calibrated selected streamgages together by calibration region.

360 **3.4.1 Individual streamgage calibration**

361 The first calibration procedure was an automated process that individually calibrated each of the
362 5,457 streamgages from the initial streamgage selection with measured streamflow (U.S.
363 Geological Survey, 2014). Results from these individual streamgage calibrations quantified the
364 ‘best’ performance of the MWBM at each gage, providing a ‘baseline’ measure for evaluation.

365 The Shuffled Complex Evolution (SCE) global-search optimization algorithm (Duan et al., 1993)
366 has been frequently used as an optimization algorithm in hydrologic studies (Hay et al., 2006;
367 Blasone et al., 2007; Arnold et al., 2012), including previous studies with the MWBM (Hay and
368 McCabe, 2010). Further details can be found in Duan et al. (1993). SCE was used to maximize a
369 combined objective function based on: (1) Nash-Sutcliffe Efficiency (NSE) coefficient using
370 measured and simulated monthly runoff and (2) NSE using natural log-transformed measured
371 and simulated runoff (logNSE), using the entire period of record for each streamgage. The NSE
372 measures the predictive power of the MWBM in matching the magnitude and variability of the
373 measured and simulated runoff (Nash and Sutcliffe, 1970). The NSE coefficient ranges from $-\infty$
374 to 1, with 1 indicating a perfect fit, and values less than 0 indicating that measured mean runoff
375 is a better predictor than model simulations. The NSE has been shown to give more weight to
376 the larger values in a time series (peak flows) at the expense of lower values (low flows)
377 (Legates and McCabe, 1999), so the logNSE was incorporated into the objective function to give
378 weight to low-flow periods (Tekleab et al., 2011).

379 **3.4.2 Grouped streamgage calibration**

380 The second calibration procedure was an automated process that calibrated groups of
381 streamgages together for each calibration region to derive a single set of MWBM parameters
382 (Table 1) for each calibration region (Fig. 6). The NSE and logNSE values from the individual
383 streamgage calibrations (described in the previous section) were used to identify streamgages
384 that should not be used for grouped streamgage calibration. If the individual streamgage
385 calibration was not ‘satisfactory’, then it was felt that it would not provide useful information for
386 the grouped streamgage calibration procedure.

387 Satisfactory individual streamgage calibrations were identified with the following procedure:

- 388 (1) Eliminate all streamgages with NSE values < 0.3 .
- 389 (2) If the number of remaining streamgages for a given calibration region is > 10 , then
 390 eliminate all streamgages with $NSE < 0.5$.
- 391 (3) If the number of streamgages for a given calibration region is > 25 , then eliminate all
 392 streamgages with $NSE_{log} < 0$.
- 393 (4) If the number of remaining streamgages for a calibration region is < 5 , check to see if any
 394 of the eliminated streamgages were reference streamgages (as defined in Falcone et al., 2010),
 395 then add the reference streamgages back in if the NSE value > 0.0 . Reference streamgages are
 396 USGS streamgages deemed to be largely free of anthropogenic impacts and flow modifications
 397 (Falcone et al., 2010; Kiang et al., 2013).

398 These criteria, while somewhat arbitrary, were chosen so that no calibration region had less than
 399 5 streamgages for the grouped streamgage calibration. Using the above criterion, of the 5,457
 400 streamgages individually calibrated, 3,125 remained as candidates for the grouped streamgage
 401 calibration procedure.

402 The grouped streamgage calibration procedure used the SCE global-search optimization
 403 algorithm with a multi-term objective function (Eq. 1). Measured and simulated values for
 404 selected streamgages contained within a calibration region were scaled to Z-scores to remove
 405 differences in magnitudes between streamgages (Eq. 2). The multi-term objective function
 406 minimized the sum of the absolute differences between Z-scores from four measured and
 407 simulated time series: mean monthly runoff (MMO, MMS), monthly runoff (MO, MS), annual
 408 runoff (AO, AS) (U.S. Geological Survey, 2014), and monthly snow water equivalent (SO, SS)
 409 for all selected streamgages within a given calibration region:

$$410 \quad \min \sum_{i=1}^n [3|MMO_i - MMS_i| + |MO_i - MS_i| + |AO_i - AS_i| + 0.5|SO_i - SS_i|] \quad (\text{Eq.1})$$

411

$$\text{where } \begin{cases} 0 & \text{if } 0.75 < SO_i - SS_i < 1.25 \\ |SO_i - SS_i| & \text{if } SS_i < SO_i^{0.75} \\ |SO_i - SS_i| & SS_i > SO_i^{1.25} \end{cases}$$

412 The measured and simulated Z-scores were calculated as:

$$413 \quad Z = (x-u)/\sigma \quad (\text{Eq. 2})$$

414 where x is the time-series value, u is the mean, and σ the standard deviation of the measured and
415 simulated variable.

416 ‘Measured’ SWE was determined for each HRU from the Snow Data Assimilation System
417 (SNODAS; National Operational Hydrologic Remote Sensing Center, 2004) and included a +/-
418 25% error bound. The unconstrained automated calibration (without a restriction on SWE) led to
419 unrealistic sources of snowmelt in the summer that enhanced the low-flow simulations. The 25%
420 error bound is arbitrary; calibrating to the actual SNODAS SWE values was found to be too
421 restrictive, but adding this error bound to the SWE values resulted in better overall runoff
422 simulations. The absolute differences of the simulated SWE Z-scores within +/- 25% of the
423 measured SWE Z-score were designated as 0. Otherwise, the absolute difference was computed
424 between the simulated SWE Z-score and either the upper or lower bounds (Eq. 1).

425 The grouped calibration procedure was run for all 110 calibration regions. For each calibration
426 region the seasonal adjustment parameters and the sensitive parameters (identified by the FAST
427 analysis -- section 3.1) were calibrated; parameters deemed not sensitive (parameter sensitivity <
428 5% of total variance) were set to their default values (see Table 1). The entire period of the
429 streamflow record for each streamgauge was split by alternating years. After calibration, mean
430 monthly measured and simulated Z-scores for runoff at all selected streamgages within a
431 calibration region were compared.

432 Figure 8 shows an example of the graphic used to evaluate the measured and simulated mean
433 monthly Z-scores for 21 streamgages selected for the region located in the Tennessee River
434 calibration region (part of NHDPlus Region R06 in Fig. 2); the orange, red, and black dots
435 indicate calibration, evaluation, and the entire period of record, respectively. A tight grouping
436 around the one-to-one line indicates good correspondence between measured and simulated Z-
437 scores. Points closer to the upper right corner of each plot represent high-flow periods. Points
438 closer to the lower left corner of the plot represent low-flow periods. Streamgages within a

439 calibration region were assigned the same parameter values; therefore streamgages that plotted
440 outside (two standard deviations) of the one-to-one line were considered to not be representative
441 of the calibration region, and the calibration procedure for that calibration region was repeated
442 without those streamgages.

443 *Figure 8. Measured versus simulated mean monthly Z-scores for the Tennessee River*
444 *calibration region (see Fig. 10b for location). Orange is calibration, red is evaluation, and*
445 *black is all years.*

446 The goal of the second calibration procedure was to find a single parameter set for each
447 calibration region. Past applications of the MWBM (Wolock and McCabe, 1999, McCabe and
448 Wolock, 2011a) used a single set of fixed MWBM parameters for the entire CONUS. Many of
449 the streamgages included in the second calibration procedure could be affected by significant
450 anthropogenic effects; the seasonal adjustment factors, calibrated at each individual streamgage,
451 could account for these effects and result in satisfactory NSE values. Streamgages that were
452 removed due to poor performance in the second calibration were assumed to have anthropogenic
453 effects not consistent with the streamgages that plotted along the one-to-one line. Poor
454 performance may result because the MWBM fails to reliably simulate runoff for a watershed
455 because of model limitations (i.e. not including all important hydrologic processes), but the
456 calibration regions are assumed to be homogeneous based on the FAST analysis. Therefore it is
457 assumed that if some of the streamgages within a region have satisfactory results, then the
458 MWBM is able to simulate runoff in that region.

459 **4 MWBM calibration region results**

460 **4.1 Individual streamgage calibration results**

461 The individual streamgage calibrations provided information regarding: (1) the potential
462 suitability of a given streamgage for inclusion in a grouped calibration, and (2) a ‘baseline’
463 measure for evaluation of the grouped calibration results. Reference and non-reference
464 streamgages were considered in this application; if the runoff at a streamgage could not be
465 calibrated individually to a ‘satisfactory’ level (based on criterion outlined in section 3.4.2), then
466 it was felt that it would not provide useful information for the grouped streamgage calibration

467 procedure. Figure 9 shows the NSE (Fig. 9a) and logNSE (Fig. 9b) coefficients from the
468 individual streamgage calibrations for the CONUS. Scattered throughout the CONUS are NSE
469 and logNSE values less than 0.0 (triangles in Fig. 9). These poor results are likely streamgages
470 with poor streamflow records, either due to measurement error or anthropogenic effects (dams,
471 water use, etc.).

472 *Figure 9. Individual streamgage calibration results: (a) Nash-Sutcliffe Efficiency (NSE)*
473 *coefficient and (b) log of the NSE (logNSE).*

474 **4.2 Grouped streamgage calibration results**

475 **4.2.1 Mean monthly z-scores**

476 Figure 10a shows a scatterplot of measured versus simulated mean monthly Z-scores for runoff,
477 similar to Figure 8, but based on all available years (the black dots in Fig. 8) for all the final
478 calibration streamgages (1,575 streamgages). Four regions are highlighted to illustrate the
479 monthly variability in MWBM results across the CONUS (see Fig. 10b for locations). The four
480 regions are: New England (67 streamgages, red); Tennessee River basin (21 streamgages,
481 orange); Platte Headwaters (15 streamgages, blue); and Pacific Northwest (33 streamgages,
482 green) (Fig. 10b).

483 *Figure 10. (a) Measured versus simulated mean monthly Z-scores for runoff at all streamgages*
484 *and (b) location of highlighted streamgages for four calibration regions: New England (67*
485 *streamgages, red); Tennessee River (21 streamgages, orange); Platte Headwaters (15*
486 *streamgages, blue); and Pacific Northwest (33 streamgages, green).*

487 In Fig. 10a, three of the regions (New England, Tennessee River, and Pacific Northwest), show
488 simulated Z-scores that correspond favorably to measured Z-scores for each of the twelve
489 months, including periods of low and high runoff. These regions represent marine or humid
490 climates with homogenous physio-climatic conditions and an even spatial distribution of
491 streamgages, where models should be expected to perform well (see Fig. 9) There is a higher
492 variability in model results for the high-flow months (May - June) for streamgages within the

493 Platte Headwaters (Fig. 10a; blue dots) than for low-flow months. This variability may be
494 related to factors controlling the magnitude and timing of snow melt runoff (Fig. 9).

495 For each calibration streamgauge, a set of four months were identified that represent different
496 parts of the measured mean monthly hydrograph (highest- and lowest- flow month and the two
497 median-flow months). The measured and simulated mean monthly streamflow Z scores
498 corresponding to the four months are plotted as cumulative frequencies (Fig. 11) to compare how
499 well the simulated Z scores matched measured Z scores for different parts of the hydrograph
500 over the entire set of calibration gages. For the highest-flow, there is an under-estimation of
501 runoff, with the greatest divergence between the two distributions in the middle to lower half of
502 the distribution (Fig. 11a). For the median-flow, the measured and simulated Z scores are well
503 matched (Fig. 11b). For the 10 lowest-flow, simulated Z scores are greater than measured Z
504 scores, with the greatest divergence between the two distributions in the middle to upper half of
505 the distribution (Fig. 11c).

506 *Figure 11. Z-score cumulative frequency for (a) highest-, (b) median-, and (c) lowest-flow*
507 *months.*

508 The median Z-score errors (simulated - measured) by region for the (a) highest-, (b) median-,
509 and (c) lowest-flows are shown in Figure 12. The largest errors are for the highest-flows (Fig.
510 12a). The MWBM simulations under-estimate the highest flows for much of the CONUS. The
511 errors for median-flows are fairly uniform and consistent across the CONUS (Fig. 12b), with a
512 median error close to 0. For the lowest-flow months the MWBM over-estimates low flows for a
513 large portion of the Midwest (Fig. 12c).

514 *Figure 12. Z-score error (simulated - measured) for (a) highest-, (b) median-, and (c) lowest-*
515 *flow months.*

516 **4.2.2 Nash-Sutcliffe efficiency**

517 Figure 13 compares the NSE from the individual streamgauge calibrations (gageNSE) with the
518 grouped calibrations (groupNSE) for all final streamgages used in the second calibration
519 procedure. NSE values > 0.75 (dashed line) and > 0.5 (solid line) indicate very good and
520 satisfactory results (Moriasi et al., 2007). Overall, most NSE values fall above the 0.5 NSE

521 threshold of satisfactory performance (median of gageNSE and groupNSE = 0.76). The gageNSE
522 values are used here as a ‘baseline’ for evaluation of the groupNSE results. The groupNSE
523 values were not expected to be greater than the gageNSE values since (1) NSE was not used as
524 an objective function in the grouped calibration, and (2) grouped calibrations found the ‘best’
525 parameter set for a set of streamgages versus an individual streamgage. Figure 13 shows an equal
526 distribution of NSE values around the one-to-one line, indicating that the grouped calibration
527 provided additional information over the individual streamgage calibrations (cases where
528 groupNSE are greater than gageNSE in Fig. 13). The difference between the gageNSE and
529 groupNSE becomes larger as the NSE values decrease, reflecting the increasing uncertainty in
530 the grouped calibrations in areas with lower gageNSE values.

531 *Figure 13. Nash Sutcliffe Efficiency from individual (gageNSE) and grouped (groupNSE)*
532 *calibration. Calibration regions in New England (67 streamgages, red); Tennessee River*
533 *(21 streamgages, orange); Platte Headwaters (15 streamgages, blue); and Pacific Northwest*
534 *(33 streamgages, green) are highlighted (see Fig. 10b for location).*

535 Four regions are highlighted in Fig. 13 to illustrate the variability of NSE across the CONUS
536 (see Fig. 10b for locations). The highlighted regions in New England (red), Tennessee River
537 (orange), and Pacific Northwest (green), show good groupNSE and gageNSE results. Four of
538 the 15 streamgages in the Platte Headwaters (blue) have groupNSE values ≤ 0.5 . This is
539 probably related to simulation error during the snowmelt period (May - June, Fig. 10a).

540 Figure 14 shows the median groupNSE by calibration region for the CONUS. The pattern is very
541 similar to that shown for the individual streamgage calibration results in Fig. 9a and highlights
542 the problem areas shown in Fig. 12.

543 *Figure 14. Median Nash Sutcliffe Efficiency (NSE) by calibration region of streamgages used*
544 *for calibration.*

545

546 **5 Discussion**

547 This study presented a parameter regionalization procedure for calibration of the MWBM,
548 resulting in an application that can be used for simulation of hydrologic variables for both gaged
549 and ungaged areas in the CONUS. The regionalization procedure grouped HRUs on the basis of
550 similar sensitivity to five model parameters. Parameter values and model uncertainty
551 information within a group was then passed from gaged to ungaged areas within that group.

552 **5.1 Regionalized parameters**

553 Results from this study indicate that regionalized parameters can be used to produce satisfactory
554 MWBM simulations in most parts of the CONUS (Fig. 13). Despite the differences between the
555 individual streamgage calibration and grouped calibration, Figure 13 illustrates that the grouped
556 calibration strategy, which focused only on sensitive parameters, can provide just as much
557 information as the individual streamgage calibration with no constraints on the parameter
558 optimization other than the default ranges. The MWBM is a simple hydrologic model as it has
559 minimal parameters, which are conceptual in nature (not physically based). It may be that this
560 type of model is best for regionalization when parameter sensitivity can be identified and HRU
561 behavior can be classified by a small number of clearly defined spatial groups. More
562 complicated models with many more interactive parameters may not respond as well to this
563 simple type of regionalization; more parameters may lead to more parameter interaction and
564 situations of equifinality which might confuse the analysis.

565 The adjustments of precipitation and temperature parameters for the individual streamgage
566 calibrations accounted for local errors such as rain gage under catch of precipitation. In addition
567 these climate adjustments also account for local anthropogenic effects on streamflow (e.g. dams,
568 diversions) since streamgages were not screened for these effects prior to individual streamgage
569 calibration. In the grouped streamgage calibrations, the same precipitation and temperature
570 adjustments are applied at every streamgage within the calibration region, making these climate
571 adjustments more of a regional adjustment and producing more of a 'reference' condition for
572 each calibration region.

573 **5.2 Parameter sensitivities and dominant process**

574 The MWBM parameter sensitivities varied by hydroclimatic index (RR and RV) and across the
575 CONUS (Fig. 4). The parameter sensitivity patterns give an indication of dominant hydrologic
576 processes based on MWBM. The dominant process can be seasonal and MWBM performance
577 may be enhanced by extending the use of SA along the temporal domain to identify and
578 temporally vary the parameters that are seasonally important to the MWBM. For example, error
579 in peak flow months is the primary cause for poor model performance in the Platte Headwaters
580 (Fig. 10). For the Platte Headwaters, the final parameter set performed well for simulated Z-
581 scores for the regionalized low- and median-flow conditions (Fig. 10a, July through April), but
582 was not able to replicate measured mean monthly flows for May and June. In this case, the
583 dominant processes controlling hydrologic behavior change with season and the parameters
584 controlling the dominant response may have to change accordingly (Gupta et al., 2008; Reusser
585 et al., 2011).

586 **5.3 Model accuracy**

587 The pattern of MWBM accuracies shown in Fig. 9 and 14 are similar to those shown by Newman
588 et al. (2015; Fig. 5a) in which a daily time-step hydrologic model was calibrated for 671 basins
589 across the CONUS. Our study and the Newman et al. (2015) study both indicate the same
590 ‘problem areas’ with the poorest performing basins generally being located in the high plains and
591 desert southwest. Newman et al. (2015) attributed variation in model performance by region to
592 spatial variations in aridity and precipitation intermittency, contribution of snowmelt, and runoff
593 seasonality.

594 The inferior MWBM results in the ‘problem areas’ can be attributed to multiple factors which
595 likely include inadequate hydrologic process representation and errors in forcing data (e.g.
596 climate data), and/or measured streamflow. Archfield et al. (2015) state that the performance of
597 continental-domain hydrologic models is considerably constrained by inadequate model
598 representation of dominant hydrologic processes. For example, the simplicity of the MWBM
599 presents limitations on the representation of deeper groundwater reservoirs, gaining and losing

600 stream reaches, simplistic AET, and the effects of surface processes (infiltration and overland
601 flow) that need to be represented at finer time steps than monthly.

602 The dominant hydrologic processes in the ‘problem areas’ appear to be poorly represented at the
603 daily (Newman et al., 2015) and monthly time steps. This may be due to inadequate forcing
604 data, the quality of which ‘is paramount in hydrologic modeling efforts’ (Archfield et al., 2015)
605 and/or the lack of ‘good’ reference streamflow data for calibration and evaluation. Both surely
606 play a role and emphasize the need for incorporation of additional datasets so that calibration and
607 evaluation of intermediate states in the hydrologic cycle are examined.

608 **6 Conclusions**

609 A parameter regionalization procedure was developed for the CONUS that transferred parameter
610 values from gaged to ungaged areas for a MWBM. The FAST global-sensitivity algorithm was
611 implemented on a MWBM to generate parameter sensitivities on a set of 109,951 HRUs across
612 the CONUS. The parameter sensitivities were used to group the HRUs into 110 calibration
613 regions. Streamgages within each calibration region were used to calibrate the MWBM
614 parameters to produce a regionalized set of parameters for each calibration region. The
615 regionalized MWBM parameter sets were used to simulate monthly runoff for the entire
616 CONUS. Results from this study indicate that regionalized parameters can be used to produce
617 satisfactory MWBM simulations in most parts of the CONUS.

618 The best MWBM results were achieved simulating low- and median-flows across the CONUS.
619 The high-flow months generally showed lower skill levels than the low- and median-flow
620 months, especially for regions with dominant seasonal cycles. The lowest MWBM skill levels
621 were found in the high plains and desert southwest and can be attributed to multiple factors
622 which likely include inadequate hydrologic process representation and errors in forcing data
623 and/or measured streamflow. Calibration and evaluation of intermediary fluxes and states in the
624 MWBM through additional measured datasets may help to improve MWBM representations of
625 these model states by helping to constrain parameterization to measured values.

626 **7 Acknowledgments**

627 This research was financially supported by the U.S. Department of Interior South Central
628 Climate Science Center (<http://southcentralclimate.org/>), U.S. Environmental Protection Agency
629 Office of Water, and the U.S. Geological Survey WaterSMART initiative. This paper is a
630 product of discussions and activities that took place at the USGS John Wesley Powell Center for
631 Analysis and Synthesis (<https://powellcenter.usgs.gov/>). Further project support was provided
632 by the Jeff Falgout of the USGS Core Science Systems (CSS) Mission Area. Any use of trade,
633 product, or firm names is for descriptive purposes only and does not imply endorsement by the
634 U.S. Government.

635

636

637

638

639

640

641

642

643

644

645

646

647 **8 References**

- 648 Adam, J.C., and Lettenmaier, D.P.: Bias correction of global gridded precipitation for solid
649 precipitation undercatch, *J. Geophys. Res.*, 108, 1-14, doi:10.1029/2002JD002499, 2003.
- 650 Ali, G., Tetzlaff, D., Soulsby, C., McDonnell, L.L., and Capell, R.: A comparison of similarity
651 indices for catchment classification using a cross-regional dataset, *Adv. Water Resources*, 40,
652 11-22, <http://dx.doi.org/10.1016/j.advwatres.2012.01.008>, 2012.
- 653 Archfield, S.A., Clark, M., Areheimer, B., Hay, L.E., McMilan, H., Kiang, J.E., Seibert, J.,
654 Bock, A., Wagener, T., Farmer, W.H., Andressian, V., Attinger, S., Viglione, A., Knight, R.,
655 Markstrom, S., and Over, T.: Improving the performance of hydrologic models across local to
656 continental domains: A discussion of research needs, *Water Resour. Res.*, 2015, In review.
- 657 Arnold, J.G., Moriasi, D.N., Gassman, P.W., Abbaspour, K.C., White, M.J., Srinivasan, R.,
658 Santhi, C., Harmel, R.D., van Griensven, A., Van Liew, M.W., Kannan, N., and Jha, M.K.:
659 SWAT: Model Use, Calibration and Validation, *T. ASABE*, 55(4), 1491-1508, 2012.
- 660 Bárdossy, A., Huang, Y., and Wagener, T.: Simultaneous calibration of hydrological models in
661 geographical space, *Hydrol. Earth Syst. Sci. Discuss.*, 12, 1123-11268, doi:10.5194/hessd-12-
662 11223-2015, 2015.
- 663 Blasone, R.-S., Madsen, H., and Rosbjerg, D.: Parameter estimation in distributed hydrological
664 modelling: comparison of global and local optimisation techniques, *Nord. Hydrol.*, 34,451-476,
665 doi:10.2166/nh.2007.024, 2007.
- 666 Blodgett, D.L., Booth, N.L., Kunicki, T.C., Walker, J.L., and Viger, R.J.: Description and
667 Testing of the Geo Data Portal: A Data Integration Framework and Web Processing Services for
668 Environmental Science Collaboration. US Geological Survey, Open-File Report 2011-1157, 9
669 pp., Middleton, WI, USA, 2011.
- 670 Blöschl, G., and Sivapalan, M.: Scale issues in hydrological modeling: a review, *Hydrol.*
671 *Process.*, 9, 251-290, 1995.

672 Blosch, G., Sivapalan, M., Wagener, T., Viglione, A., and Savenije, H (Eds.): *Runoff Prediction*
673 in *Ungauged Basins: Synthesis across Processes, Places, and Scales*. Cambridge University
674 Press, Cambridge, England, 2013.

675 Clark, M.P., and Slater, A.G.: *Probabilistic Quantitative Precipitation Estimation in Complex*
676 *Terrain*, *B. Am. Meterol. Soc.*, 7, 3-2, doi: <http://dx.doi.org/10.1175/JHM474.1>, 2006.

677 Cukier, R.I., Fortuin, C.M., Shuler, K.E., Petschek, A.G, and Schaibly, J.H: *Study of sensitivity*
678 *of coupled reaction systems to uncertainties in rate coefficients 1*, *J. Chem. Phys.*, 59(8), 3873-
679 3878, 1973.

680 Cukier, R.I., Schiably, J.H., and Shuler, K.E: *Study of sensitivity of coupled reaction systems to*
681 *uncertainties in rate coefficients 3*, *J. Chem. Phys.*, 63(3), 1140-1149, 1975.

682 Cuo, L., Giambelluca, T.W., and Ziegler, A.D: *Lumped parameter sensitivity analysis of a*
683 *distributed hydrological model within tropical and temperate catchments*, *Hydrol. Process.*,
684 25(15), 2405-2421, doi:10.1002/hyp.8017, 2011.

685 Duan, Q., Gupta, V.K., and Sorooshian, S.: *A shuffled complex evolution approach for effective*
686 *and efficient optimization*, *J. Optimiz. Theory App.*, 76, 501-521, doi:10.1007/BF00939380,
687 1993.

688 Falcone, J.A., Carlisle, D.M., Wolock, D.M., and Meador, M.R.: *GAGES: A stream gage*
689 *database for evaluating natural and altered flow conditions in the conterminous United States*,
690 *Ecology*, 91, p. 621, A data paper in *Ecological Archives E091-045-D1*, available at
691 <http://esapubs.org/Archive/ecol/E091/045/metadata.htm> (last accessed 15 November 2012),
692 2010.

693 Farnsworth, R.K., Thompson, E.S., and Peck, E.L.: *Evaporation Atlas for the Contiguous 48*
694 *United States*, NOAA Technical Report NWS 33, 41 pp., National Oceanic and Atmospheric
695 Administration, Washington, D.C., 1982.

696 Groisman, P.Y., and Legates, D.R.: *The accuracy of United States precipitation data*, *Bull. Am.*
697 *Meterol. Soc.*, 75(2), 215-227, doi:10.1029/1998JD200110, 1994.

698 Gupta, H.V., Wagener, T., Liu, Y.Q. "Reconciling theory with observations: Elements of
699 diagnostic approach to model evaluation." *Hydrologic Processes* (2008): 22,3802-3813.

700 Guse, B., Reusser, D.E., and Fohrer, N.: How to improve the representation of hydrological
701 processes in SWAT for a lowland catchment - temporal analysis of parameter sensitivity and
702 model performance, *Hydrol. Process.*, 28(4), 2561-2670, doi:10.1002/hyp.9777, 2013.

703 Hay, L.E., Leavesley, G.H., Clark, M.P., Markstrom, S.L., Viger, R.J., and Umemoto, M.: Step-
704 wise multiple-objective calibration of a hydrologic model for a snowmelt-dominated basin, *J.*
705 *Am. Water Resour. A.*, 42(4), 877-890, doi:10.1111/j.1752-1688.2006.tb04501.x, 2006.

706 Hay, L.E., and McCabe, G.J.: Spatial Variability in Water-Balance Model Performance in the
707 Conterminous United States, *J. Am. Water Resour. Ass.*, 38(3), 847-860, DOI: 10.1111/j.1752-
708 1688.2002.tb01001.x, 2002.

709 Hay, L.E., and McCabe, G.J.: Hydrologic effects of climate change in the Yukon River Basin,
710 *Climate Change*, 100, 509-523, doi:10.1007/s10584-010-9805-x, 2010.

711 Kapangaziwiri, E., Hughes, D. A., and Wagener, T.: Constraining uncertainty in hydrological
712 predictions for ungauged basins in southern Africa, *Hydrol. Sci. J.*, 57, 1000–1019, 5
713 doi:10.1080/02626667.2012.690881, 2012.

714 Kiang, J.E., Stewart, D.W., Archfield, S.A., Osborne, E.B., and Eng, K.: A National Streamflow
715 Network Gap Analysis. U.S. Geological Survey, Scientific Investigative Reports 2013-5013, 94
716 pp., Reston, VA, USA, 2013.

717 Kirchner, J.W.: Getting the right answers for the right reasons: Linking measurements,
718 analyses, and models to advance the science of hydrology, *J. Hydrol.*, 42, W03S04,
719 doi:10.1029/2005WR004362, 2006.

720 Kokkonen, T.S., Jakeman, A.J., Young, P.C., and Koivusalo, H.J.: Predicting daily flows in
721 ungauged catchments: model regionalization from catchment descriptors at the Coweeta
722 Hydrologic Laboratory, North Carolina, *Hydrol. Process.*, 17, 2219-2238, doi:10.1002/hyp.1329,
723 2003.

724 Krause, P., Doyle, D. P., and Bäse, F.: Comparison of different efficiency criteria for
725 hydrological model assessment, *Adv. Geosci.*, 5, 89–97, doi:10.5194/adgeo-5-89-2005, 2005.

726 Legates, D.R., and McCabe, G.J.: Evaluating the use of “goodness-of-fit” Measures in
727 hydrologic and hydroclimatic model validation, *Water Resour. Res.*, 35(1), 233-241,
728 doi:10.1029/1998WR900018, 1999.

729 Maurer, E.P., Wood, A.W., Adam, J.C., Lettenmaier, D.P., and Nijssen, B.: A long-term
730 hydrologically-based data set of land surface fluxes and states for the conterminous United
731 States, *J. Climatol.*, 15, 3237-3251, [http://dx.doi.org/10.1175/1520-](http://dx.doi.org/10.1175/1520-0442(2002)015<3237:ALTHBD>2.0.CO;2)
732 [0442\(2002\)015<3237:ALTHBD>2.0.CO;2](http://dx.doi.org/10.1175/1520-0442(2002)015<3237:ALTHBD>2.0.CO;2), 2002.

733 McCabe, G.J., Hay, L.E., Bock, A., Markstrom, S.L., and Atkinson, D.R.: Inter-annual and
734 spatial variability of Hamon potential evapotranspiration model coefficients, *J. Hydrol.*, 521,
735 389-394, doi:10.1016/j.jhydrol.2014.12.006, 2015.

736 McCabe, G.J., and Markstrom, S.L.: A Monthly Water-Balance Model Driven By a Graphical
737 User Interface. U.S. Geological Survey Open-File Report 2007-1008, 12 pp., Reston, VA, USA,
738 2007.

739 McCabe, G.J., and Wolock, D.M.: Century-scale variability in global annual runoff examined
740 using a water balance model, *Int. J. Climatol.*, 31, 1739-1748, doi:10.1002/joc.2198, 2011a.

741 McCabe, G.J., and Wolock, D.M.: Independent effects of temperature and precipitation on
742 modeled runoff in the conterminous United States, *Water Resour. Res.*, 47, W1152,
743 doi:10.1029/2011WR010630, 2011b.

744 McManamay, R.A., Orth, D.J., Dolloff, C.A., and Frimpong, E.A: Regional Frameworks
745 applied to Hydrology: Can Landsapes-based frameworks capture the hydrologic variability?,
746 *River Res. App.*, 28, 1325-1339, doi:10.1002/rra.1535, 2011.

747 Merz, R., and Blöschl, G.: Regionalisation of catchment model parameters, *J. Hydrol.*, 287, 95-
748 123, doi:10.1016/j.jhydrol.2003.09.028, 2004.

749 Moriasi, D.N, Arnold, J.G., Van Liew, M.W., Bingner, R.L., Harmel, R.D., and Vieth, T.L.:
750 Model Evaluation Guidelines for Systematic Quantification of Accuracy in Watershed
751 Simulations, T. ASABE, 50, 885-900, 2007.

752 Nash, J.E., and Sutcliffe, J.V.: River flow forecasting through conceptual models Part I: a
753 discussion of principles, J. Hydrol., 10, 282-290, doi:10.1016/0022-1694(70)90255-6, 1970.

754 National Operational Hydrologic Remote Sensing Center, Snow data Assimilation System
755 (SNODAS) Data Products at the NSIDC, 9/30/2003 through 6/13/2014, National Snow and Ice
756 Data Center, Boulder, Colorado, USA, <http://dx.doi.org/10.7265/N5TB14TC>, 2004.

757 Newman, A.J., Clark, M.P., Sampson, K., Wood, A., Hay, L.E., Bock, A., Viger, R.J., Blodgett,
758 D., Brekke, L., Arnold, J.R., Hopson, T., and Duan, Q.: Development of a large-sample
759 watershed-scale hydrometeorological data set for the contiguous USA: data set characteristics
760 and assessment of regional variability in hydrologic model performance, Hydrol. Earth Syst. Sc.,
761 19, 209-223, doi:10.5194/hess-19-209-2015, 2015.

762 Oudin, L., Andreassian, V., Perrin, C., Michel, C., and Le Moine, N.: Spatial proximity,
763 physical similarity, regression and ungaged catchments: a comparison of regionalization
764 approaches based on 913 French catchments, Water Resour. Res., 44, 1-15,
765 doi:10.1029/2007WR006240, 2008.

766 Oudin, L., Kay, A., Andreassian, V., and Perrin, C.: Are seemingly physically similar
767 catchments truly hydrologically similar?, Water Resour. Res., 46, W11558,
768 doi:10.1029/2009WR008887, 2010.

769 Oyler, J.W., Dobrowski, S.Z., Ballantyne, A.P., Klene, A.E., and Running, S.W.: Artificial
770 amplification of warming trends across the mountains of the western United States, Geophys.
771 Res. Lett., 42, 153-161, doi:10.1002/2014GL062803, 2015.

772 Peel, M.C., Chiew, F.H.S., Western, A.W., and McMahon, T.A.: Extension of unimpaired
773 monthly streamflow data and regionalization of parameter values to estimate streamflow in

774 ungauged catchments. Report to National Land and Water Resources Audit, Center for
775 Environmental Application and Hydrology, University of Melbourne, Parkville, 2000.

776 Qamar, M.U., Ganora, D., and Claps, P.: Monthly Runoff Regime Regionalization Through
777 Dissimilarity-Based Methods, *Water Resour. Manag.*, 29, 4735-4751, doi:10.1007/s11269-015-
778 1087-7, 2015.

779 R Core Team: R: A language and environment for statistical computing, R Foundation for
780 Statistical Computing, Vienna, Austria, 2013.

781 Reusser, D.: fast: Implementation of the Fourier Amplitude Sensitivity Test (FAST), R package
782 version, <http://CRAN.R-project.org/package=fast>, (last access: 9 April 2014), 2012.

783 Reusser, D., Buytaert, W., and Zehe, E.: Temporal dynamics of model parameter sensitivity for
784 computationally expensive models with the Fourier amplitude sensitivity test, *Water Resour.*
785 *Res.*, 47, W07551, doi:10.1029/2010WR009947, 2011.

786 Saltelli, A., Tarantola, S., and Campolongo, F.: Sensitivity analysis as an ingredient of
787 modeling, *Stat. Sci.*, 15, 377-395, 2000.

788 Samuel, J., Coulibaly, P., and Metcalfe, R.A.: Estimation of Continuous Streamflow in Ontario
789 Ungauged Basins: Comparison of Regionalization Methods, *J. Hydrol. Eng.*, 16, 447-459,
790 [http://dx.doi.org/10.1061/\(ASCE\)HE.1943-5584.0000338](http://dx.doi.org/10.1061/(ASCE)HE.1943-5584.0000338), 2011.

791 Sankarasubramanian, A., and Vogel, R.M.: Hydroclimatology of the continental United States,
792 *Geophys. Res. Lett.*, 30, 1-4, doi:10.1029/2002GL015937, 2003.

793 Santhi, C., Kannan, N., Arnold, J.G., and Luzio, D.: Spatial calibration and temporal validation
794 of flow for regional scale hydrologic modeling, *J. Am. Water Resour. Ass.*, 4, 829-846,
795 doi:10.1111/j.1752-1688.2008.00207.x, 2008.

796 Sawicz, K., Wagener, T., Sivapalan, M., Troch, P.A., and Carrillo, G.: Catchment classification:
797 empirical analysis of hydrologic similarity based on catchment function in the eastern USA,
798 *Hydrol. Earth Syst. Sc.*, 15, 2895-2911, 2011.

799 Sefton, C.E.M., and Howarth, S.M.: Relationships between dynamic response characteristics
800 and physical descriptors of catchments in England and Wales, *J. Hydrol.*, 211, 11-16,
801 doi:10.1016/S0022-1694(98)00163-2, 1998.

802 Seibert, J.: Regionalization of parameters for a conceptual rainfall runoff model, *Agr. Forest*
803 *Meteorol.*, 98-99, 279-293, doi:10.1016/S0168-1923(99)00105-7, 1999.

804 Smakhtin, V.Y.: Low flow hydrology: a review, *J. Hydrol.*, 240, 147-186, doi:10.1016/S0022-
805 1694(00)00340-1, 2001.

806 Tang, Y., Reed, P., Wagener, T., and van Werkhoven, T.: Comparing sensitivity analysis
807 methods to advance lumped watershed model identification and evaluation, *Hydrol. Earth Syst.*
808 *Sc.*, 11, 793-817, 2007.

809 Tekleab, S., Uhlenbrook, S., Mohamed, Y., Savenije, H.H.G., Temesgen, M., and Wenninger, J.:
810 Water balance modeling of Upper Blue Nile catchments using a top-down approach, *Hydrol.*
811 *Earth Syst. Sci.*, 15, 2179-2193, doi:10.5194/hess-15-2179-2011, 2011.

812 Troch, P.A., Paniconi, C., and McLaughlin, D.: Catchment-scale hydrological modeling and
813 data assimilation, *Adv. Water Resour.*, 26, 131-135, doi:10.1016/S0309-1708(02)00087-8, 2003.

814 USEPA (United States Environmental Protection Agency) and USGS (United States Geological
815 Survey): NHDPlus User Guide, available at [ftp://ftp.horizon-](ftp://ftp.horizon-systems.com/NHDPlus/documentation/NHDPLUS_UserGuide.pdf)
816 [systems.com/NHDPlus/documentation/NHDPLUS_UserGuide.pdf](ftp://ftp.horizon-systems.com/NHDPlus/documentation/NHDPLUS_UserGuide.pdf) (last access 12 Nov 2014),
817 2010.

818 US Geological Survey: A National Water Information System, available at: [http://waterdata.](http://waterdata.usgs.gov/nwis/)
819 [usgs.gov/nwis/](http://waterdata.usgs.gov/nwis/) (last access 27 March 2014), 2014.

820 Van Griensven, A., Meixner, T., Grunwald, S., Bishop, T., Diluzio, and M., Srinivasan, R.: A
821 global sensitivity analysis tool for the parameters of multi-variable catchment models, *J. Hydrol.*,
822 324, 10-23, doi:10.1016/j.jhydrol.2005.09.008, 2006.

823 Vandewiele, G.L., and Elias, A.: Monthly water balance of ungaged catchments obtained by
824 geographical regionalization, *J. Hydrol.*, 170, 277-291, doi:10.1016/0022-1694(95)02681-E,
825 1995.

826 Viger, R., Bock, A.: GIS Features of the Geospatial Fabric for National Hydrologic Modeling,
827 U.S. Geological Survey, Denver, CO, USA, doi:10.5066/F7542KMD, 2014.

828 Vogel, R.M.: Regional calibration of watershed models, *Watershed Models*, Singh, V.P., and
829 Frevert, D.F. (Eds.), CRC Press, Boca Raton, FL, USA, 2006.

830 Vrugt, J.A., ter Braak, C.J.F., Clark, M.P., Hyman, J.M., Robinson, B.A.: Treatment of input
831 uncertainty in hydrologic modeling: Doing hydrology backwards with Markov Chain Monte
832 Carlo simulation, *Water Resour. Res.*, 44, W00B09, doi:10.1029/2007WR006720, 2008.

833 Wolock, D.M.: STATSGO soil characteristics for the conterminous United States. U.S.
834 Geological Survey Open-File Report 1997-656, Reston, VA, USA, available at:
835 <http://water.usgs.gov/GIS/metadata/usgswrd/XML/muid.xml>, (last access 3 March 2012), 1997.

836 Wolock, D.M., and McCabe, G.J.: Explaining spatial variability in mean annual runoff in the
837 conterminous United States, *Clim. Res.*, 11, 149-159, doi:10.3354/cr011149, 1999.

838 Zhang, X., Srinivasan, R., and Van Liew, M.: Multi-Site Calibration of the SWAT Model for
839 Hydrologic Modeling, *T. ASABE*, 51, 2039-2049, 2008.

840

841

842

843

844

845

846

847

848

849

Parameter	Definition	Range	Default
1. <i>Drofac</i>	Controls fraction of precipitation that becomes runoff	0, 0.10	0.05
2. <i>Rfactor</i>	Controls fraction of surplus that becomes runoff	0.10, 1.0	0.5
3. <i>Tsnow</i>	Threshold above which all precipitation is rain (°C)	-10.0, -2.0	-4.0
4. <i>Train</i>	Threshold below which all precipitation is snow (°C)	0.0, 10.0	7.0
5. <i>Meltcoef</i>	Proportion of snowpack that becomes runoff	0.0, 1.0	0.47
6. <i>Ppt_adj</i>	Seasonal adjustment factor for precipitation (%)	0.5, 2.0	1
7. <i>Tav_adj</i>	Seasonal adjustment for temperature (°C)	-3.0, 3.0	0

850

851

Table 1. Monthly Water Balance Model parameters and ranges.

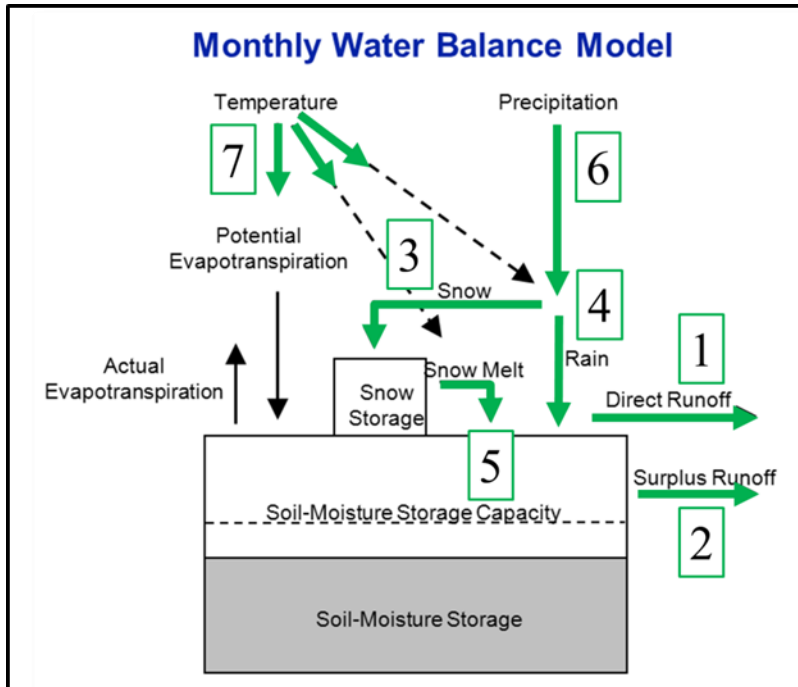
852

853

854

855

856



857

858 Figure 1. Conceptual diagram of the Monthly Water Balance Model (McCabe and Markstrom
 859 2007). Processes influenced by model parameters used in Fourier Amplitude Sensitivity Test
 860 (FAST) are identified by green arrow and numbered (Table 1).

861

862

863

864

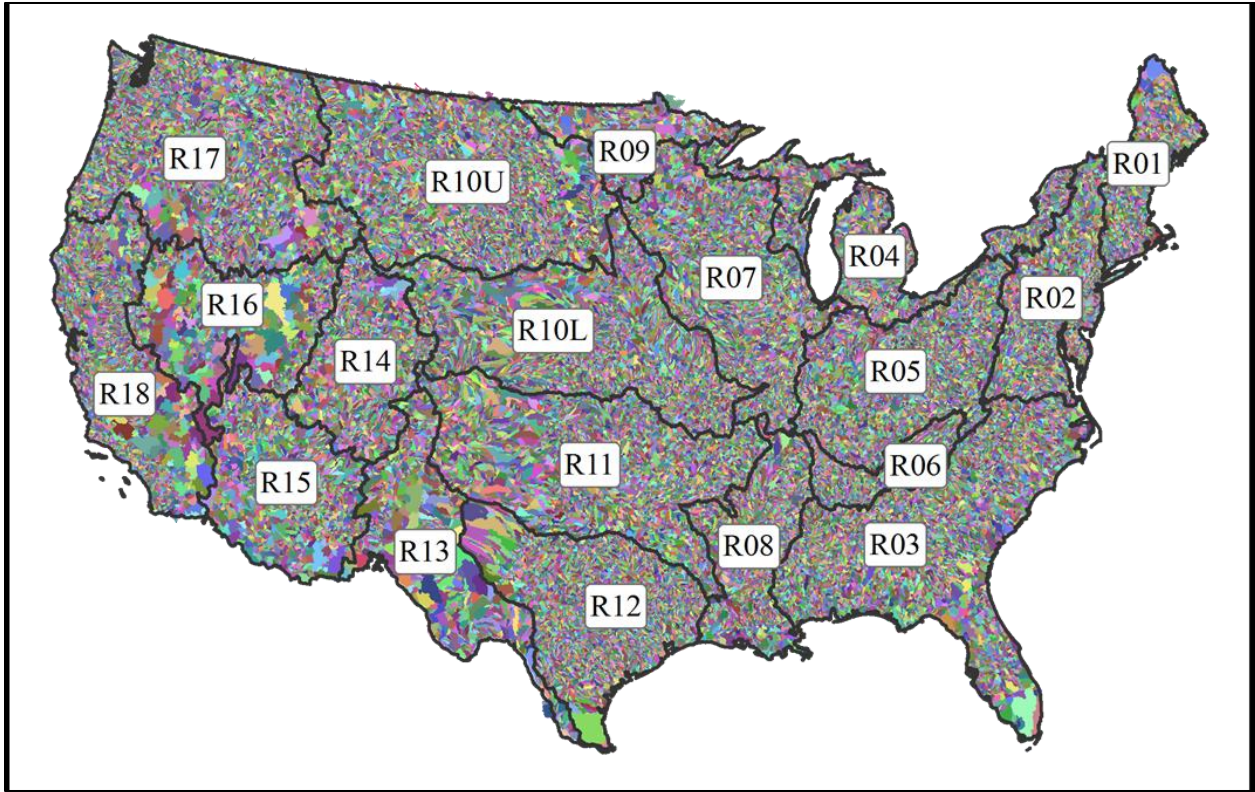
865

866

867

868

869



870

871 Figure 2. Hydrologic Response Units of the Geospatial Fabric, differentiated by color, overlain
872 by NHDPlus region boundaries (R01-R18).

873

874

875

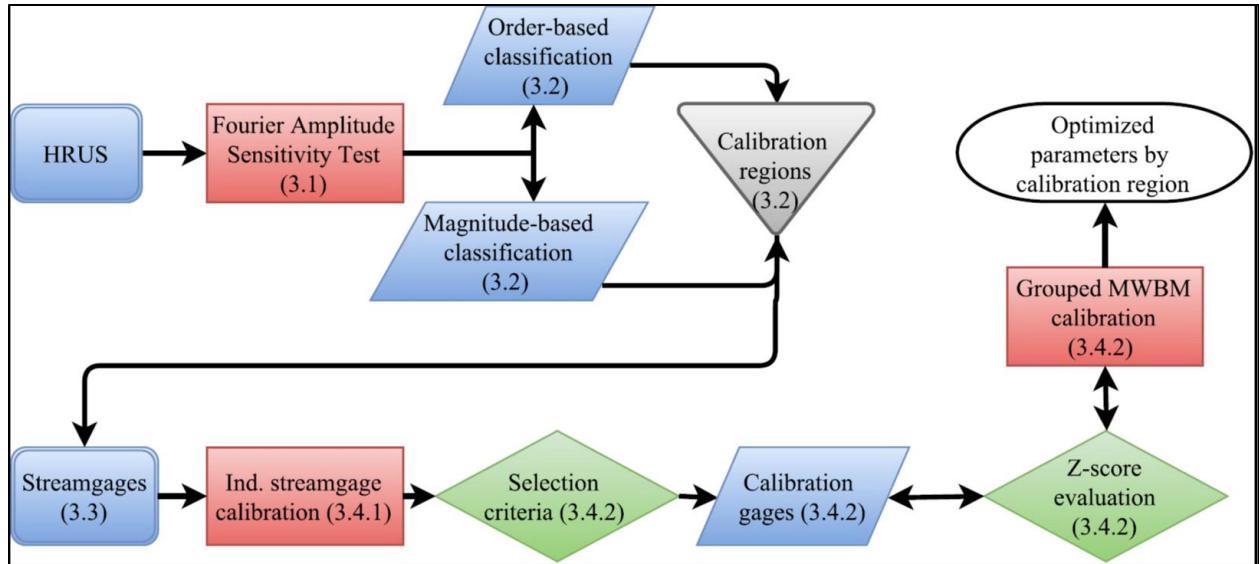
876

877

878

879

880



881

882 Figure 3. Schematic flowchart of the parameter sensitivity analysis and regionalization method
 883 described in this paper (Section 3).

884

885

886

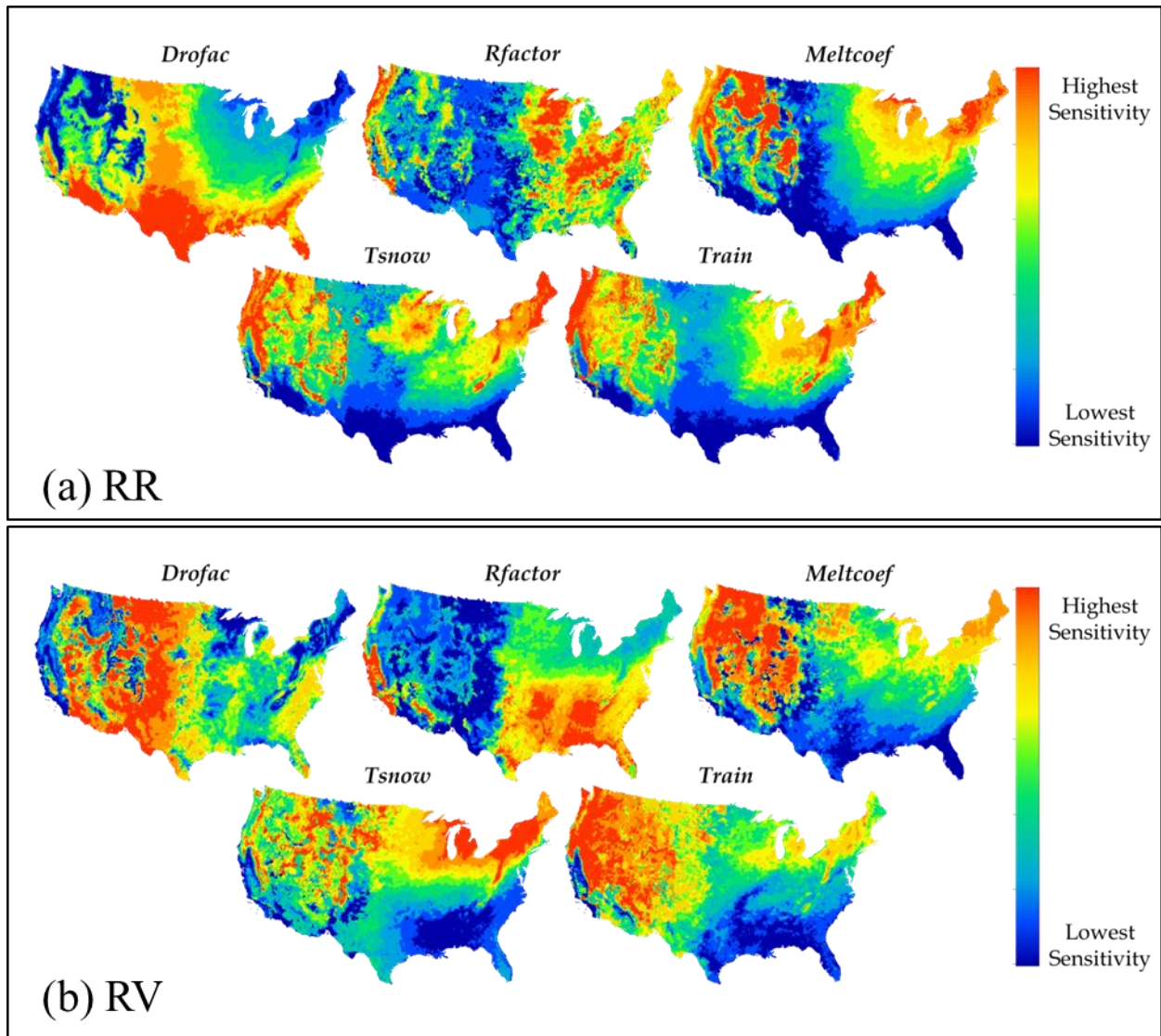
887

888

889

890

891



892

893 Figure 4. Relative sensitivity of the (a) Rainfall Ratio (RR) and (b) Runoff Variability (RV)

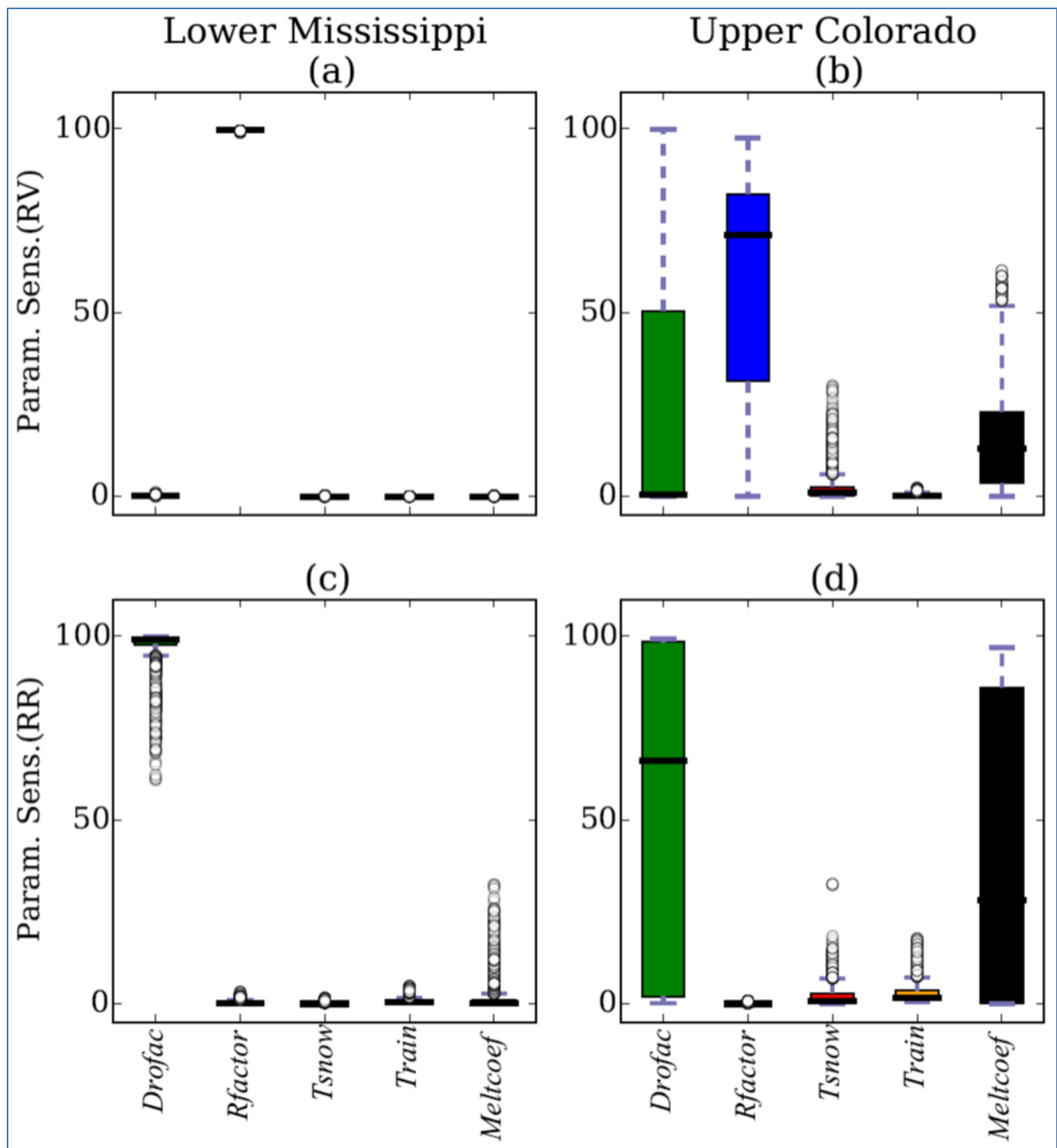
894

indices to Monthly Water Balance Model parameters.

895

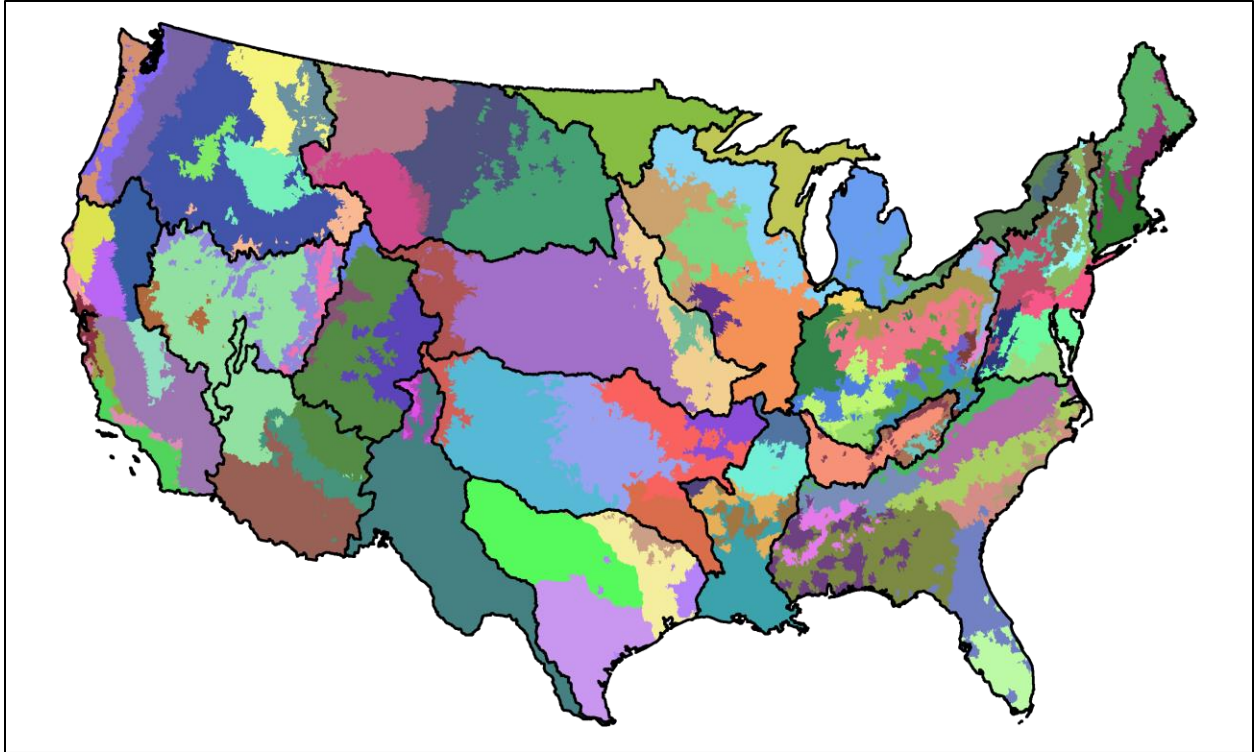
896

897



898
 899 Figure 5. Parameter sensitivities of Runoff Variability (RV; a and b) and Runoff Ratio (RR; c
 900 and d) indices for Monthly Water Balance Model parameters in the Lower Mississippi (R08) and
 901 Upper Colorado (R14).

902



903

904 Figure 6. Final 110 Monthly Water Balance Model calibration regions differentiated by colors.
905 A subset of streamgages within each calibration region were calibrated in a group-wise fashion
906 to produce a single optimized parameter set for the entire region (Fig. 3).

907

908

909

910

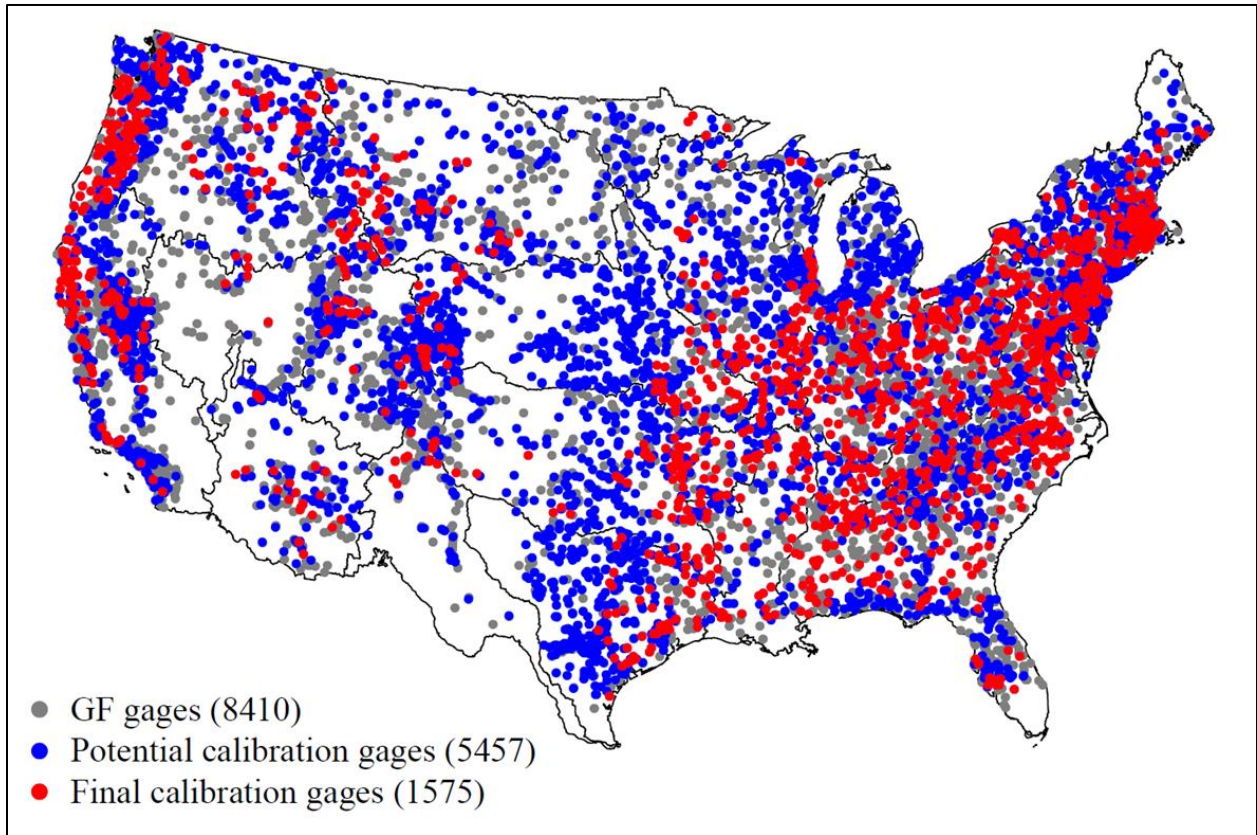
911

912

913

914

915



916

917 Figure 7. Streamgages tested in the study. GF notes geospatial fabric for national hydrologic
918 modeling (Viger and Bock, 2014).

919

920

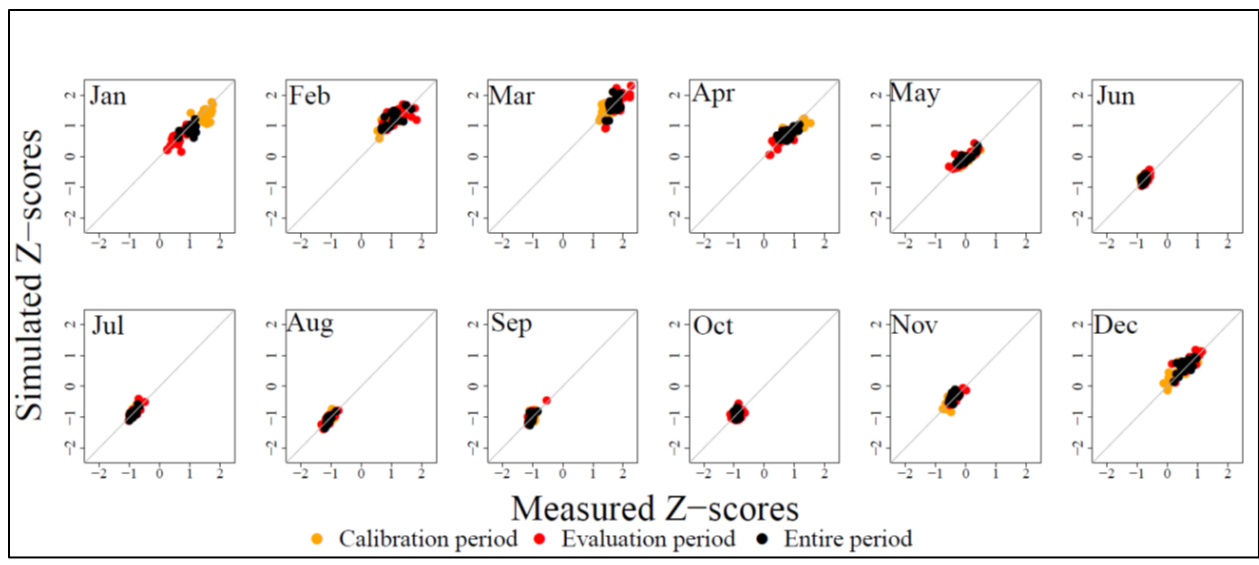
921

922

923

924

925



926

927 Figure 8. Measured versus simulated mean monthly Z-scores for the Tennessee River calibration
 928 region (see Fig. 10b for location). Orange is calibration, red is evaluation, and black is all years.

929

930

931

932

933

934

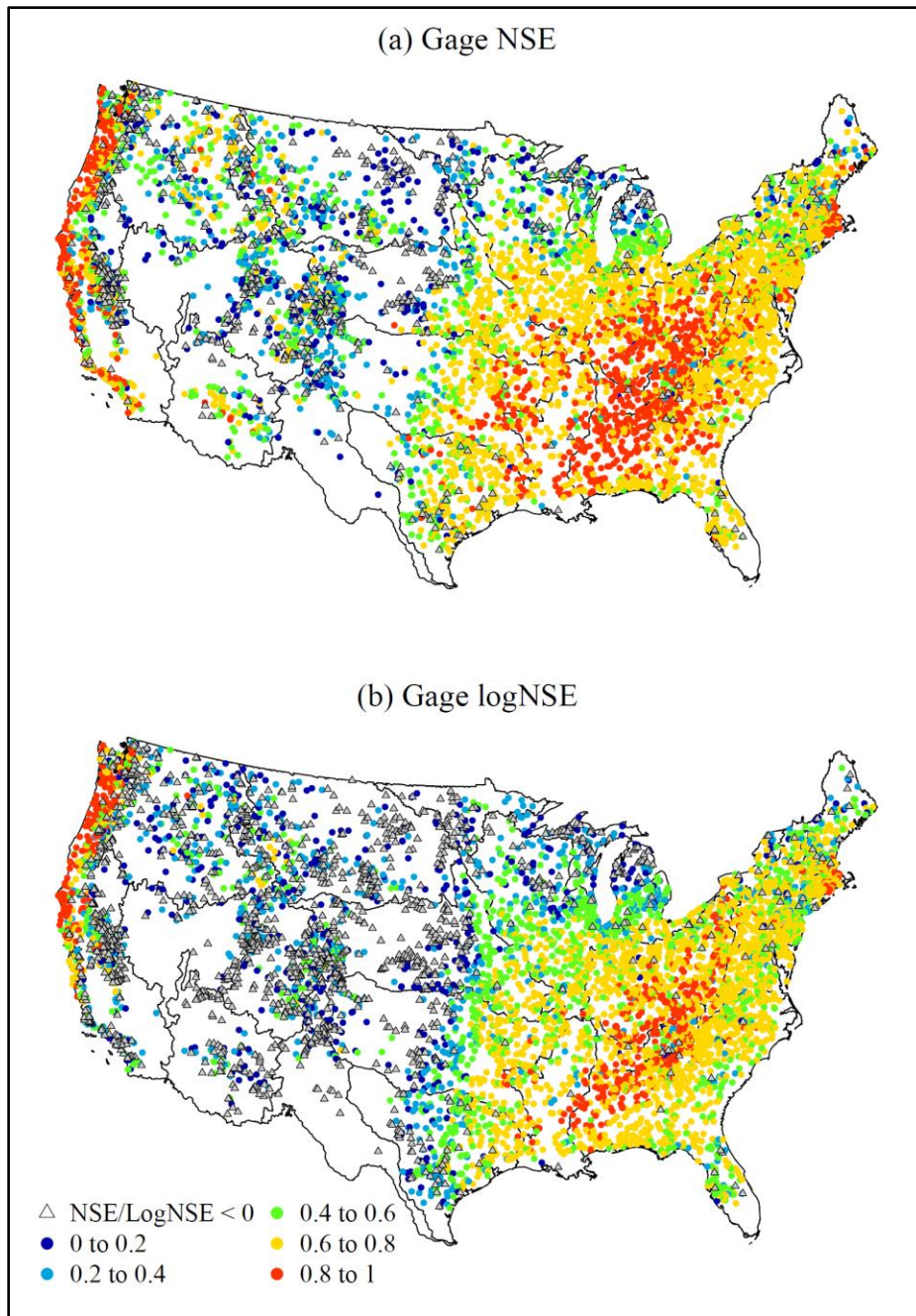
935

936

937

938

939

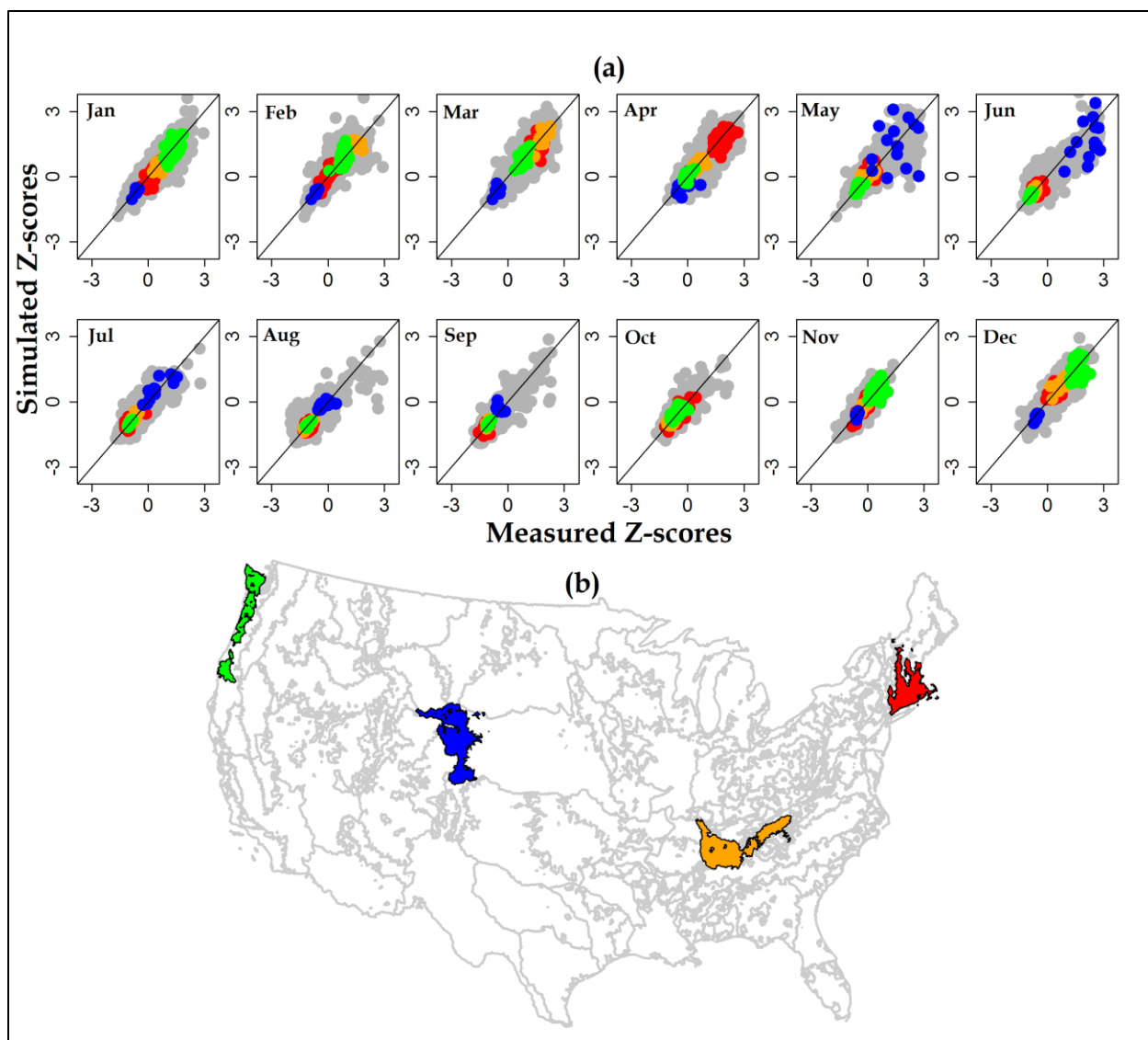


940

941 Figure 9. Individual streamgage calibration results: (a) Nash-Sutcliffe Efficiency (NSE)
 942 coefficient and (b) log of the NSE (logNSE).

943

944



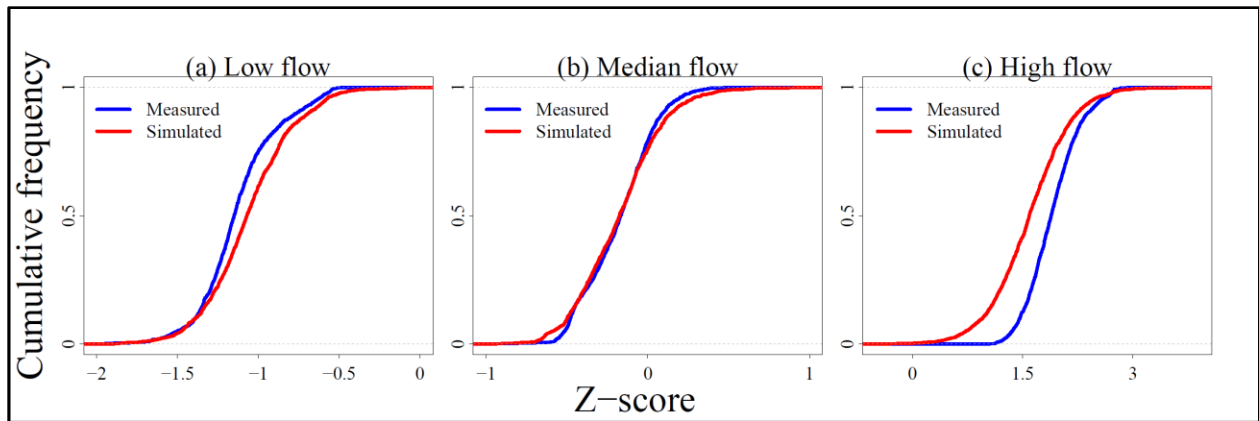
945

946 Figure 10. (a) Measured versus simulated mean monthly Z-scores for runoff at all streamgages
 947 and (b) location of highlighted streamgages for four calibration regions: New England (67
 948 streamgages, red); Tennessee River (21 streamgages, orange); Platte Headwaters (15
 949 streamgages, blue); and Pacific Northwest (33 streamgages, green).

950

951

952



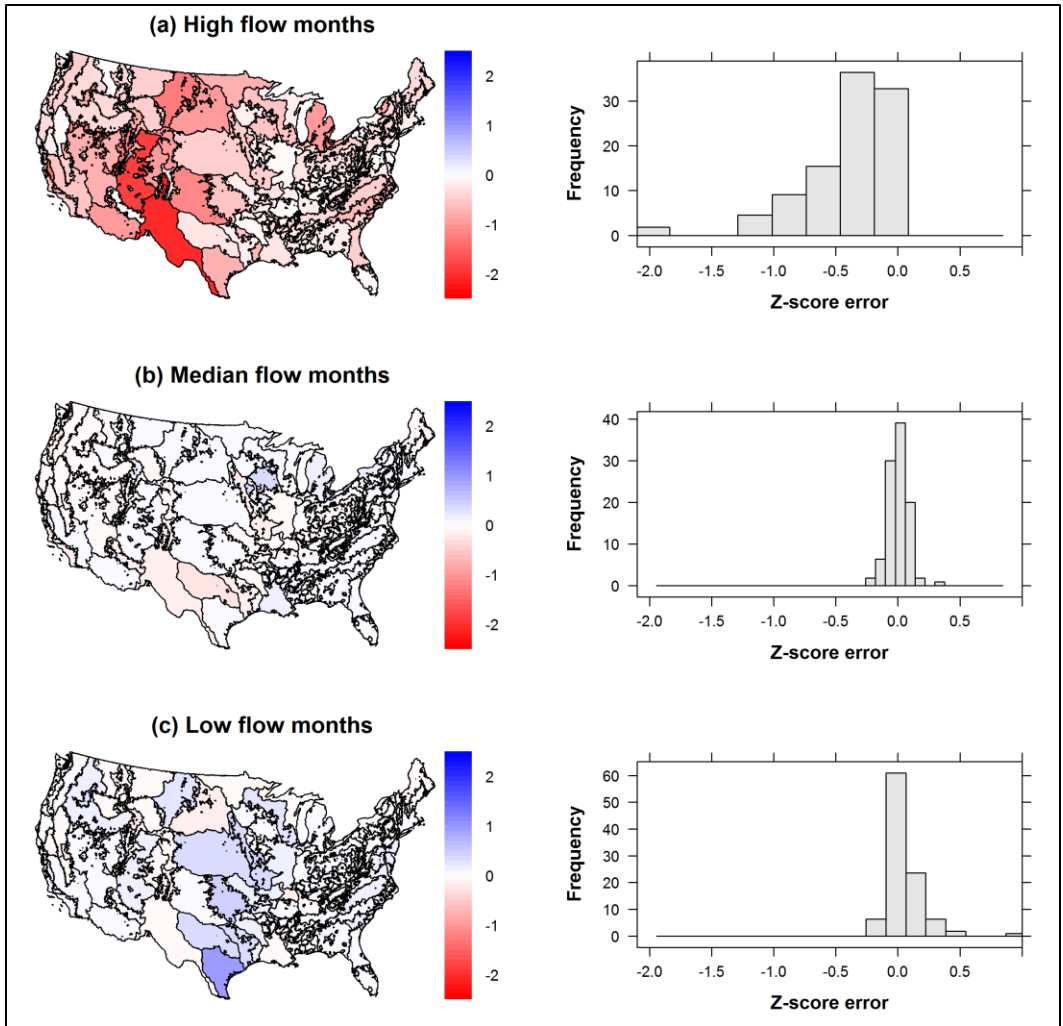
953

954 Figure 11. Z-score cumulative frequency for (a) highest-, (b) median-, and (c) lowest-flow

955

months.

956



957

958 Figure 12. Z-score error (simulated - measured) for (a) highest-, (b) median-, and (c) lowest-
 959 flow months.

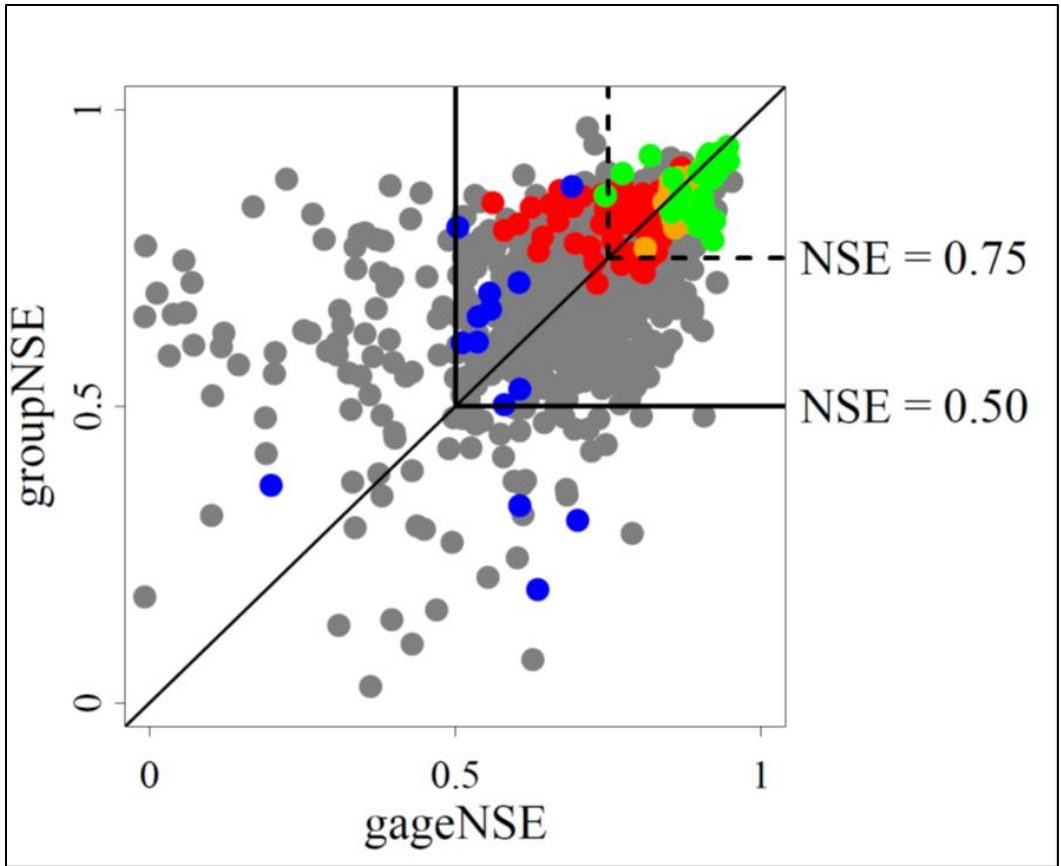
960

961

962

963

964



965

966

Figure 13. Nash Sutcliffe Efficiency from individual (gageNSE) and grouped (groupNSE) calibration. Calibration regions in New England (67 streamgages, red); Tennessee River (21 streamgages, orange); Platte Headwaters (15 streamgages, blue); and Pacific Northwest (33 streamgages, green) are highlighted (see Fig. 10b for location).

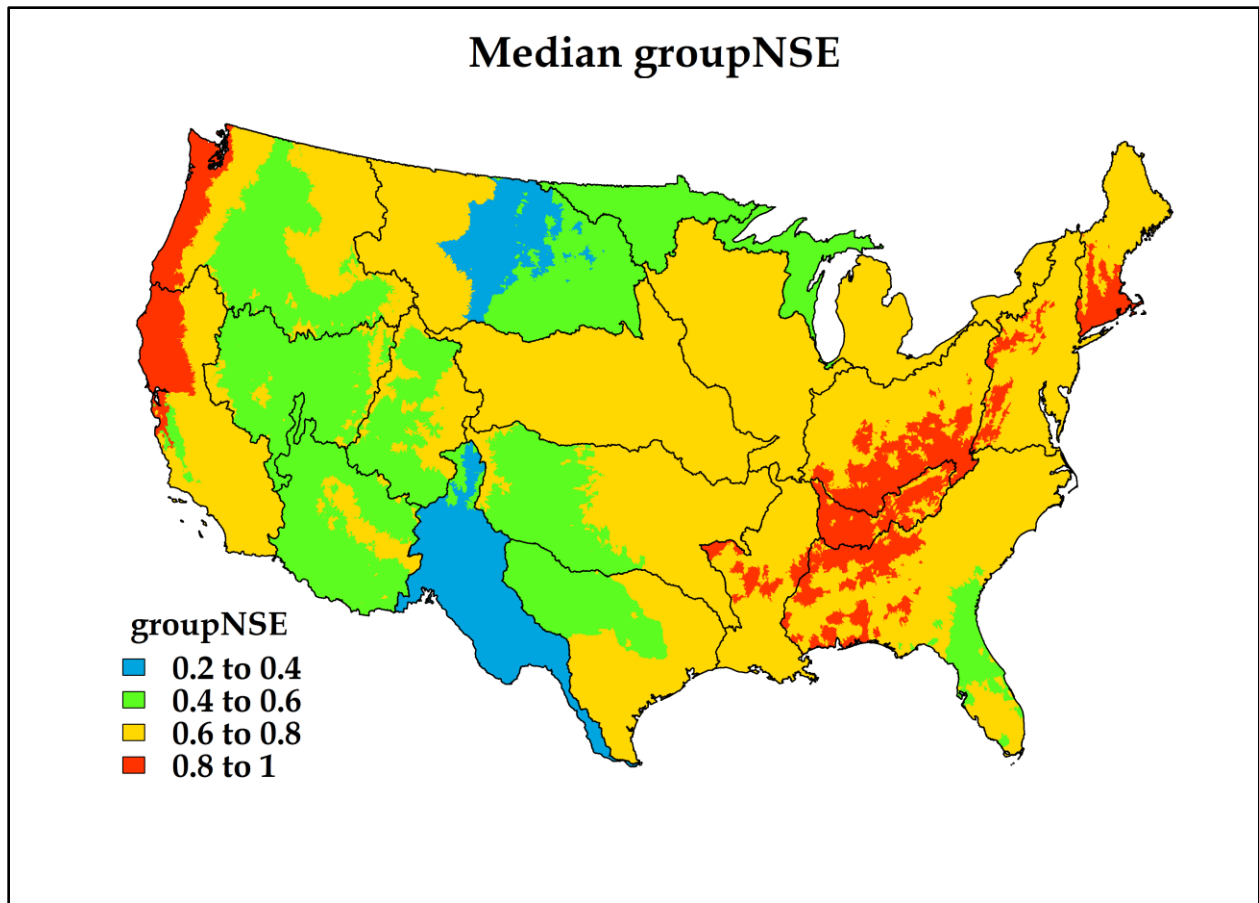
970

971

972

973

974



975

976 Figure 14. Median Nash Sutcliffe Efficiency (NSE) by calibration region of streamgages used for
977 calibration.

978

979